USGS
science for a changing world

Prepared in cooperation with California Department of Water Resources

# Using the STARS Model to Evaluate the Effects of Two Proposed Projects for the Long-Term Operation of the State Water Project Incidental Take Permit Application and CEQA Compliance

Open-File Report 2019–1127
Version 2.0, February 2020

U.S. Department of the Interior
U.S. Geological Survey

# Using the STARS Model to Evaluate the Effects of Two Proposed Projects for the Long-Term Operation of the State Water Project Incidental Take Permit Application and CEQA Compliance

By Russell W. Perry, Amy C. Hansen, Scott D. Evans, and Tobias J. Kock

**Prepared in cooperation with California Department of Water Resources**

Open File Report 2019–1127
Version 2.0, February 2020

**U.S. Department of the Interior**
**U.S. Geological Survey**

**U.S. Department of the Interior**
DAVID L. BERNHARDT, Secretary

**U.S. Geological Survey**
James Reilly II, Director

U.S. Geological Survey, Reston, Virginia
First release: 2019
Revised: February 2020 (ver. 2.0)



**Suggested citation:**
Perry, R.W., Hansen, A.C., Evans, S.D., and Kock, T.J., 2019, Using the STARS Model to evaluate the effects of two proposed projects for the long-term operation of State Water Project Incidental Take Permit Application and CEQA compliance (ver. 2.0, February 2020): U.S. Geological Survey Open-File Report 2019-1127, 39 p. plus appendixes, https://doi.org/10.3133/ofr20191127.

ISSN 2331-1258 (online)

# Contents



# Figures

# Conversion Factors

Inch/Pound to International System of Units

| Multiply | By | To obtain |
|---|---|---|
| | Volume | |
| acre-foot (acre-ft) | 1,233 | cubic meter ($m^3$) |
| | Flow rate | |
| cubic foot per second ($ft^3/s$) | 0.02832 | cubic meter per second ($m^3/s$) |

International System of Units to Inch/Pound

| Multiply | By | To obtain |
|---|---|---|
| | Length | |
| kilometer (km) | 0.6214 | mile (mi) |

# Abbreviations

| | |
|---|---|
| CEQA | California Environmental Quality Act |
| CESA | California Endangered Species Act |
| CVP | Central Valley Project |
| DCC | Delta Cross Channel |
| DSM2 | Delta Simulation Model II |
| DWR | California Department of Water Resources |
| EIR | Environmental Impact Report |
| ESA | Endangered Species Act |
| EX | existing |
| ITP | Incidental Take Permit |
| MCMC | Markov Chain Monte Carlo |
| NMFS | National Marine Fisheries Service |
| PP | proposed project |
| PP2b | proposed project 2b |
| STARS | Survival, Travel time, And Routing Simulation |
| SWP | State Water Project |
| USFWS | U.S. Fish and Wildlife Service |
| USBR | U.S. Bureau of Reclamation |
| USGS | U.S. Geological Survey |
| WY | water year |
| WYI | water year index |

# Using the STARS Model to Evaluate the Effects of Two Proposed Projects for the Long-Term Operation of the State Water Project Incidental Take Permit Application and CEQA Compliance

By Russell W. Perry, Amy C. Hansen, Scott D. Evans, and Tobias J. Kock

## Abstract

The California Department of Water Resources (DWR) requested analysis of juvenile Chinook salmon survival in the Sacramento-San Joaquin River Delta (henceforth identified as "the Delta") as part of an effects analysis that will be included in an Incidental Take Permit (ITP) Application. This application is in compliance with the California Endangered Species Act (CESA) and Environmental Impact Report (EIR), which is itself in compliance with California Environmental Quality Act (CEQA). DWR is seeking an ITP and preparing CEQA compliance documentation for long-term operation of the State Water Project (SWP). DWR requested assistance from the U.S. Geological Survey to aid in determining the effect of two proposed projects on juvenile Chinook salmon (*Oncorhynchus tshawytscha*) populations migrating through the Delta. Therefore, in this report we analyzed an 82-year time series of simulated river flows and Delta Cross Channel (DCC) gate operations under three scenarios constructed for the ITP: the proposed project (PP), the second proposed project (PP2b) and the existing (EX) scenarios.

To evaluate the proposed projects (PP and PP2b), we used the STARS model (Survival, Travel time, And Routing Simulation model), a stochastic, individual-based simulation model designed to predict survival of a cohort of fish that experience variable daily river flows during migration through the Delta. The STARS model uses parameter estimates from a Bayesian mark-recapture model that jointly estimates travel time and survival in eight discrete reaches of the Delta and migration routing at two key river junctions.

By applying the STARS model to the three 82-year scenarios, we found that both proposed projects had negative effects on survival, travel time, and routing in November but slightly positive effects in October, December, and May, and in June for only the PP. In November, there was a high probability that survival for PP and PP2b were less than EX and that travel time and routing to the Interior Delta for PP and PP2b were greater than for EX. We found that the magnitude of the difference in survival between scenarios was large in some years. For example, survival under both the PP and PP2b scenarios were 10 percent lower than EX in 25 percent of the water years in November. During this period, inflow to the Delta tended to be lower under the PP and PP2b scenarios, and the DCC gate was open more frequently under the PP and PP2b scenarios relative to the EX scenario. Lower inflow reduces survival, and more frequent operation of the DCC gate 1) increases the proportion of fish entering the Interior Delta, where survival is low, and thus 2) reduces survival in the Sacramento River in reaches downstream of the DCC. In contrast, during October, December, May (both PP and PP2b), and June (PP only), survival was slightly higher, travel times were lower, and routing to the Interior Delta was lower under the PP and PP2b relative to the EX scenario in the same time period, although the magnitude of the increase was relatively small in most years (less than two

percent). This difference between scenarios was driven by higher river flows in some years under the PP and PP2b relative to the EX scenario. Overall, the differences in survival, travel time, and routing distance between the three operational scenarios were primarily driven by the timing and magnitude of the annual high river flows.

## Introduction

The California Department of Water Resources (DWR) and U.S. Bureau of Reclamation (USBR) have joint responsibility for the coordinated long-term operation of the Central Valley Project (CVP) and State Water Project (SWP) in California's Central Valley. The CVP and SWP are a system of reservoirs, dams, and hydraulic and water-conveyance structures that are operated for the purposes of generating power and delivering water for agricultural and domestic use, while providing flood protection and protecting water quality for downstream users (USBR, 2019). Because the Sacramento and San Joaquin watersheds harbor several critically endangered species listed under the Endangered Species Act (ESA), USBR has undertaken consultation regarding the requirements of Section 7 of the ESA with the U.S. Fish and Wildlife Service (USFWS) and National Marine Fisheries Service (NMFS). NMFS issued a Biological Opinion in 2009 (NMFS, 2009) concluding that the long-term operations of the CVP and SWP were likely to jeopardize the continued existence of the Sacramento River Winter-Run Chinook salmon (*Oncorhynchus tshawytscha*), Central Valley Spring-Run Chinook salmon, Central Valley steelhead (*Oncorhynchus mykiss*), the Southern distinct population segment of North American green sturgeon (*Acipenser medirostris*), and the Southern resident distinct population segment of the killer whale (*Orcinus orca*).

The U.S. Geological Survey (USGS) is providing technical services to assist the DWR South Delta Branch of the Bay-Delta Office and Division of Environmental Services, Office of Regulatory Compliance and Office of Environmental Compliance, with analysis of juvenile Chinook salmon survival in the Sacramento-San Joaquin River Delta (henceforth, "the Delta") as part of an effects analysis that will be included in an Incidental Take Permit (ITP) Application in compliance with the California Endangered Species Act (CESA) and Environmental Impact Report (EIR) in compliance with California Environmental Quality Act (CEQA). DWR is seeking an ITP and preparing CEQA compliance documentation for long-term operation of the SWP. We initially conducted survival, travel-time, and routing simulations for two scenarios, the existing (EX; operations currently used) and proposed project (PP; operations proposed for use in the future), to provide through-Delta survival and travel-time distributions for a cohort of 500 individual fish entering the Delta at Freeport on each day of an 82-year daily time series of Delta inflows. The PP scenario differed from the EX scenario in the minimum flow requirements downstream of Keswick Dam, American River operations, Fall X2, Sacramento-San Joaquin Delta water quality standards, San Joaquin River inflow/export ratio, combined flow in the Old and Middle River, WIIN wetness table, Head of the Old River Barrier Gate, water quality at Vernalis, and the Stanilaus River Basin, and monthly SWP export estimates (Aaron Miller, DWR, written commun., January 21, 2020). After this report was published in November of 2019, DWR asked for an additional analysis of the proposed project 2b scenario (PP2b) in December of 2019 and this document was modified in February 2020. The PP2b scenario differed from the PP scenario in the San Joaquin River inflow/export ratio, combined flow in the Old and Middle River, WIIN wetness table, monthly SWP export estimates, SWP delivery logic, and SWP August export cut (Aaron Miller, DWR, written commun., January 21, 2020). The summaries of the 82-year simulation period can be used to identify the potential effects of SWP operations over a long-term period.

We simulated through-Delta survival under various scenarios for juvenile Chinook salmon by using results of hydrologic- and hydrodynamic-model simulations prepared by DWR. We used the STARS model (Survival, Travel time, And Routing Simulation model), a stochastic, individual-based simulation model designed to predict survival of a cohort of fish that experience varying daily river

flows as they migrate through the Delta (fig. 1). The parameters on which the STARS model is based were derived from a Bayesian mark-recapture model that jointly estimated reach-specific travel time, migration routing, and survival of juvenile Chinook salmon. This model extends the work of Perry and others (2010) to estimate the effect of the Delta Cross Channel (DCC; see $C_4$ in fig. 1) and Delta inflows as measured in the Sacramento River at Freeport (USGS streamgage 11447650; see $A_2$ in fig. 1) on survival, travel time, and routing of juvenile Chinook salmon in eight reaches of the Delta (fig. 1). Perry and others (2018) determined that the median travel time was related to the inflow in all reaches of the Delta. In contrast, survival was strongly related to inflow in only three of eight reaches (reaches 3, 4 and 5 in fig. 1). In the three reaches that exhibited strong inflow-survival relationships, river flows changed from tidally influenced, bidirectional flow at low net inflow to unidirectional downstream flow as net inflows increased, and tidal forcing was dampened. Thus, in these three reaches, route-specific survival through the Delta increased with flow, yet fish that entered the Interior Delta (reach 8 in fig. 1) through Georgiana Slough or the DCC experienced lower route-specific survival than fish that entered through other migration routes. In addition, Perry and others (2018) determined that the proportion of fish entering the Interior Delta increased as 1) inflows decreased below about 25,000 $ft^3/s$ or 2) when the DCC gate was opened (Perry and others, 2018). These mechanisms increase the proportion of fish experiencing low-survival migration routes and thereby further reducing overall survival through the Delta.

Although the effect of river flow on overall survival through the Delta has been established for some time (Newman and Rice, 2002; Newman, 2003; Perry, 2010), our goal was to use the recently developed survival, travel time, and routing relationships (Perry and others, 2018) to better understand the potential magnitude of the effect of the proposed action on juvenile salmon survival, travel time, and migration routing. Because our model incorporates the effects of river flow and DCC-gate operation on juvenile Chinook survival, travel time, and migration routing, our analysis can be used to identify mechanisms by which operations affect overall survival throughout the Delta. One drawback, however, is that the statistical model of Perry and others (2018) did not include water exports (that is, water pumped out of the Southern Delta). Thus, the modeling results in this report are insensitive to any difference in exports among the scenarios being considered. Although we are currently developing models that include export effects, those models were not available for this analysis.

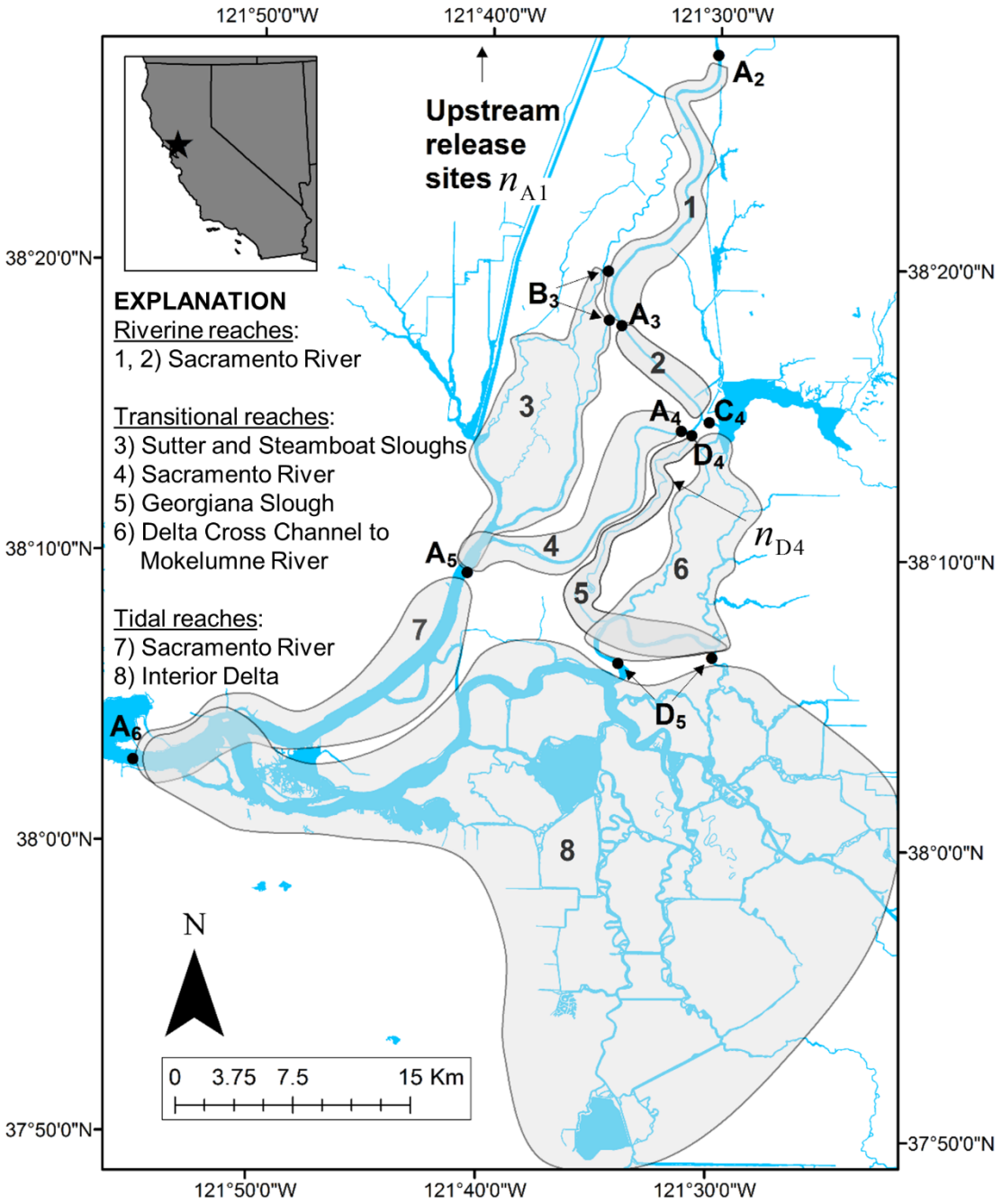


**Figure 1.** Map showing locations of acoustic-telemetry receiving stations (filled black circles) used to detect acoustic-tagged juvenile Chinook salmon as they migrated through the Sacramento-San Joaquin River Delta, northern California. Telemetry stations are labeled by migration route (A, Sacramento River; B, Sutter and Steamboat Sloughs; C, Delta Cross Channel; D, Georgiana Slough) and sampling occasion (1–8, sites 1 and 7 not shown on map). These telemetry stations divide the Delta into eight discrete reaches (shown by numbered shaded regions), with an additional reach upstream of telemetry station $A_2$ (Reach 0) used as an acclimation reach to allow fish to recover from post-release handling. Route-specific survival begins at $A_2$ (Freeport) and ends at $A_6$ (Chipps Island). Release sites are labeled as $n_{A1}$ and $n_{D4}$.

# Methods

## Model Description

Here we provide a summary of the STARS model and the associated Bayesian mark-recapture model we used to simulate survival, travel time, and migration routing for juvenile Chinook salmon in the Central Valley.

### Summary of the Bayesian Mark-Recapture Model

The STARS model uses parameter estimates from a Bayesian mark-recapture model that jointly estimates travel time and survival in eight discrete reaches of the Delta and migration routing at two key river junctions (fig. 1, stations $A_3$ and $B_3$ and stations $A_4$, $D_4$, and $C_4$). The data for the analysis consisted of 2,170 acoustic-tagged late-fall Chinook salmon released during a 5-year period (2007–11) over a wide range of Sacramento River inflows (6,816–76,986 $ft^3/s$ at Freeport (site $A_2$)). This analysis was based on acoustic telemetry data from several published studies in which interested readers can find more detail (Perry and others, 2010, 2013; Michel and others, 2015).

Although numerous studies have identified a relation between Delta inflows and survival at the Delta-wide scale, the goal of the Perry and others (2018) analysis was to quantify how the flow-survival relation varied spatially among different regions of the Delta. To quantify the reach-specific relation between river inflows and survival, they used time-varying individual covariates in which an individual's covariate value was defined as the daily mean flow of the Sacramento River at Freeport and at the DCC gate position on the day that *i*th fish entered the *n*th reach. Because of missing covariate values for undetected fish, they implemented the multistate mark-recapture model of Perry and others (2010) by using a complete data likelihood approach in a Bayesian framework (King and others, 2010). To account for missing covariate values, they jointly modeled reach-specific travel times, routing, and survival. Their analysis used the estimated parameters of a log-normal travel-time distribution for each reach to estimate travel times of undetected fish, which in turn allowed missing covariate values to be based on the estimated arrival time in a given reach. Markov Chain Monte Carlo (MCMC) techniques were used to integrate over the missing covariate values by sampling missing travel times on each iteration of the Markov chain.

Perry and others (2018) found that the proportion of fish using each migration route depended on river flow, but the direction of the relationship differed among river junctions (fig. 2). At the junction of the Sacramento River with Sutter and Steamboat Sloughs ($B_3$ in fig. 1), the probability of fish entering Sutter and Steamboat sloughs increased with river flow. In contrast, at the junction of the Sacramento River with Georgiana Slough ($D_4$ in fig. 1) and the DCC ($C_4$ in fig. 1), the probability of fish entering Georgiana Slough decreased with increasing flow. Opening the DCC gates decreased the probability of fish entering Georgiana Slough but increased the proportion of fish entering the Interior Delta through both the DCC and Georgiana Slough.

In their analysis, Perry and others (2018) also identified a negative relation between river inflows and median travel times in all reaches of the Delta (fig. 3), but the nature of the relationship between flow and survival varied among reaches (see fig. 6 in Perry and others, 2018). In the upper reaches of the Delta (reaches 1 and 2 in fig. 1), survival was consistently high regardless of inflow, whereas in the strongly tidal reaches (reaches 7 and 8 in fig. 1), there was no significant relation between river inflows and reach-specific survival despite a relation between inflow and travel time. The strongest positive flow-survival relations were identified in the three reaches that transition from river-dominated to tidally dominated flows (reaches 3, 4, and 5 in fig. 1).

The product of reach-specific survival for a given migration pathway between Freeport ($A_2$ in fig. 1) and Chipps Island ($A_6$ in fig. 1) yields the probability of surviving through each migration route at a given river discharge. Route-specific survival for all routes increased with river discharge but approached an asymptote, leveling off at about 0.75 for the Sacramento River and Sutter and Steamboat Sloughs, and at about 0.35 for fish entering Georgiana Slough when river discharges increased to more than about 30,000 $ft^3/s$ (fig. 4). The reach-specific survival relations indicate that the asymptote in route-specific survival was driven by survival in the strongly tidal reaches (reaches 7 and 8) because survival for all other reaches approached 1 as flow increased but remained constant with flow for the strongly tidal reaches. Expected travel-time distributions for each migration route decreased as river flow increased, with migration routes leading to the Interior Delta (Georgiana Slough and the Delta Cross Channel) having longer travel times than other routes (fig. 3).

The statistical relationships arising from the fitting of the Bayesian mark-recapture model reflect the expected patterns based on the hydrodynamics of the Delta. The routing patterns are consistent with what would be expected because of the structure of the water velocity across the water column and fish distributions in the channel cross section (Perry and others, 2014). Increasing inflow to the Delta dampens tidal fluctuations and increases water velocities, which in turn increase juvenile-salmon migration rates (Zabel, 2002). The flow-dependent patterns of survival rates can be qualitatively explained by the interplay between the flow, the channel topography and morphology, tidal dynamics, and predator-encounter rate (Perry and others, 2018). Thus, although the model is based on statistical relationships, the patterns on survival, travel time, and routing predicted by the STARS model are largely consistent with our expectations based on the physical principles of hydrodynamics.

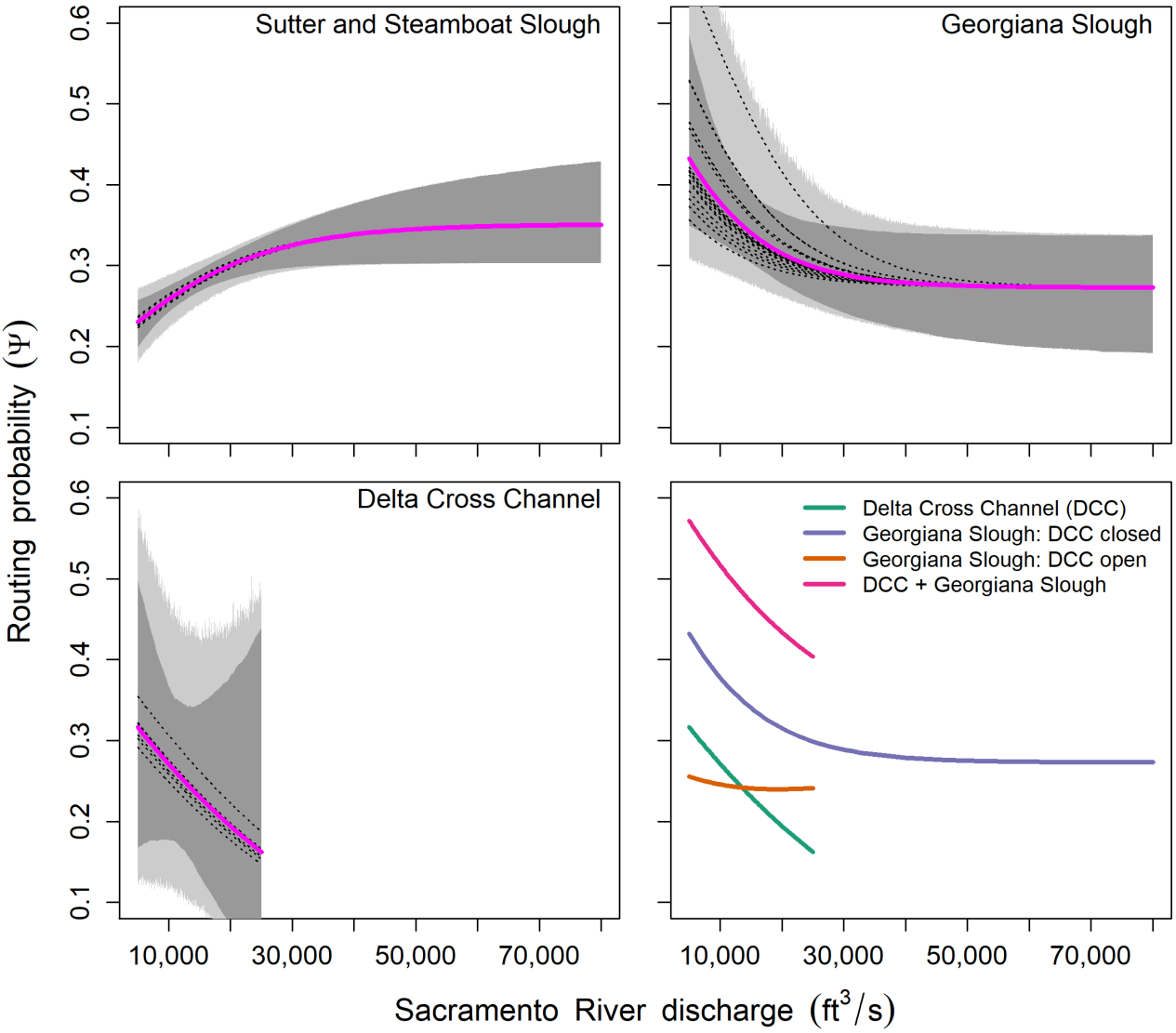


**Figure 2.** Relationships between routing probability and inflow to the Delta as measured at the Sacramento River at Freeport ($A_2$ in Fig. 1). Routing probability is defined as the probability of a fish entering a given migration route conditional on surviving to the entry point of that route. The lower right panel shows the effect of Delta Cross Channel (DCC) gate position on routing probabilities at the junction of the Sacramento River, Delta Cross Channel, and Georgiana Slough ($A_4$, $C_4$, and $D_4$ in Fig. 1), plotted at the posterior median of the parameters. Other panels show mean routing relationships (solid heavy magenta line), random-effects estimates for each release group (dotted lines), 95-percent credible interval about the mean relationship (dark gray region), and 95-percent confidence interval among release groups (light gray region). $ft^3/s$, cubic foot per second

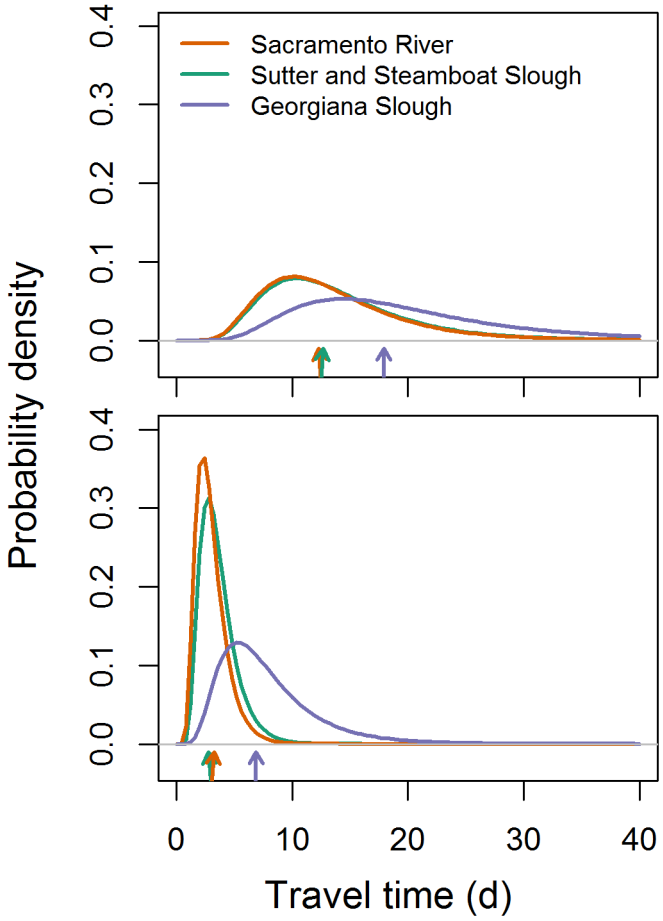


**Figure 3.** Graphs showing route-specific travel-time distributions of juvenile Chinook salmon at the 5th (top graph) and 95th (bottom graph) percentiles of discharge based on the historical flow record (8,290 and 47,910 $ft^3/s$), between Freeport and Chipps Island (see fig. 1), Sacramento-San Joaquin River Delta, northern California. Graphs were based on posterior medians of parameters for reach-specific travel-time distributions and the assumption that the Delta Cross Channel gates are closed. Colored arrows show the median travel time for each migration route. d, days

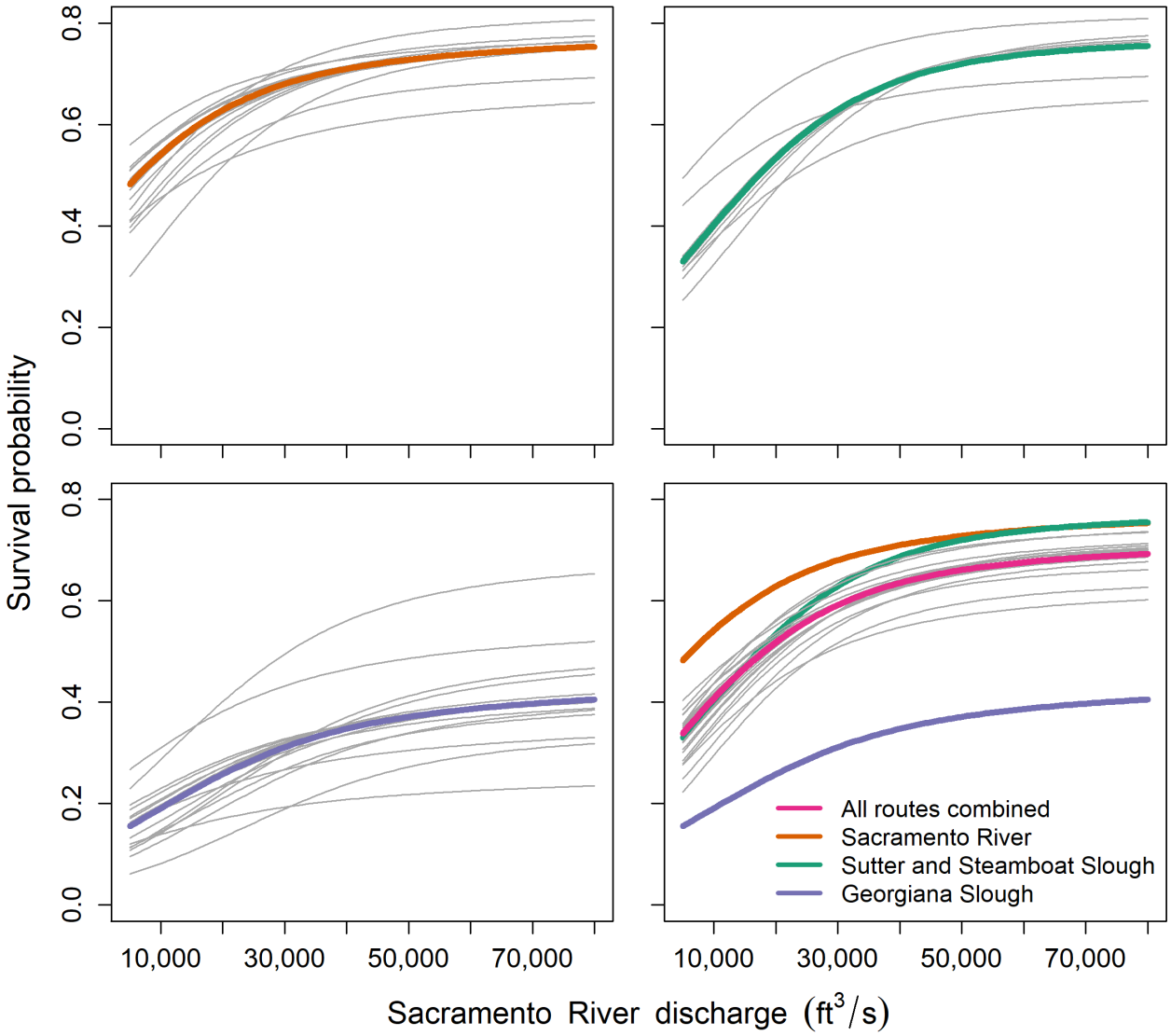


**Figure 4.** Graphs showing route-specific survival of juvenile Chinook salmon between Freeport and Chipps Island (see fig. 1) through the Sacramento-San Joaquin River Delta, northern California. Route-specific survival probabilities based on posterior-median parameter values were calculated as the products of reach-specific survival probabilities for reaches that trace each unique migration route through the Delta (shown for closed Delta Cross Channel gates). Top graphs and bottom left graph show the mean relation for each route, with thin gray lines showing the random-effect estimates for each release group. Bottom right graph compares the route-specific survival probabilities and includes survival for all routes combined. $ft^3/s$, cubic foot per second

## STARS: Survival, Travel Time, and Routing Simulation

To simulate survival, travel time, and routing, we used the results from the Bayesian mark-recapture model of Perry and others (2018). To incorporate measures of uncertainty in our simulations, we used the joint posterior distribution of the survival, routing, and travel-time parameters from the Bayesian analysis. Uncertainty was propagated by doing one simulation for each MCMC draw forming the joint posterior distribution of the parameters.

Random-effect terms in this model estimated the deviation of each release cohort from the average survival, routing, and travel-time relations; however, because we were interested in simulating new cohorts of fish, we drew new random effects for each posterior draw from a normal distribution with mean 0 and standard deviations of $\xi_S$, $\xi_\Psi$, and $\xi_\mu$ (see Perry and others, 2018, for more detail). In this way, each draw of the joint posterior distribution represents a possible state of nature in which river flow and DCC gate operations affect travel time, routing, and survival of a given cohort of fish. When comparing alternative scenarios (EX, PP, and PP2b), we used the same set of random-effect draws for both scenarios because we envisioned that the same cohort of fish was migrating through the Delta but under two possible alternative operational scenarios.

Given a daily time series of river flow and DCC gate operations, the STARS model simulates survival, migration routing, and travel time as follows (see Perry and others (2018) for the mathematical expressions associated with this algorithm):

1. Select parameter set *i* from the joint posterior distribution.
2. Initiate the simulation with 1,000 fish at Freeport on day *t*.
3. Calculate survival in reach 1 given discharge on day *t* and parameter set *i*.
4. Determine individual travel times through reach 1 from a lognormal distribution in which the mean of the distribution depends on parameter set *i* and discharge on day *t*. This yields a distribution of individual arrival times at the junction of Sutter and Steamboat Sloughs and the Sacramento River ($A_3$ and $B_3$ in fig. 1).
5. Next, draw the route taken by each fish by using a Bernoulli distribution where the probability of entering Sutter and Steamboat Sloughs is a function of parameters set *i* and discharge on the day when each fish arrives at the junction.
6. Calculate the survival probability of each individual fish in the next reach downstream given the discharge on the day when each fish entered the reach.
7. Now, draw travel times for each individual fish for the next downstream reach given the flows on the day each fish entered the reach.
8. For fish remaining in the Sacramento River, draw the route taken by fish at the junction of the Sacramento River with the DCC and Georgiana Slough ($A_4$, $C_4$, and $D_4$ in fig. 1) from a multiple Bernoulli distribution in which the probability of fish entering each route depends on the position of the DCC gates and discharge on the day each fish arrives at the junction.
9. Repeat steps 4 and 6 for all remaining reaches.
10. Repeat steps 2–9 for all days in the daily time series.
11. Repeat steps 1–10 for all iterations of the joint posterior distribution.

This simulation procedure yields a posterior predictive distribution of reach-specific survival probabilities, reach-specific travel times, and routing probabilities for a cohort of 1,000 individual fish entering the Delta at Freeport on each day of a daily time series. By using this approach, our simulation emulated the effects of daily-flow variation on through-Delta survival, travel time, and routing for a cohort of fish that entered the Delta on a given day. For example, although two cohorts may enter the Delta under identical flows at Freeport, the survival rates and travel times of these cohorts would differ if one cohort entered during an ascending hydrograph and another cohort entered during a descending hydrograph. To see an implementation of the STARS model, we encourage

readers to visit National Oceanic Atmospheric Administration's Central Valley Acoustic Tagging Website, where the STARS model is currently being used to simulate travel time, survival, and routing in real-time for the current water year (https://oceanview.pfeg.noaa.gov/shiny/FED/CalFishTrack/).

## Comparing the Proposed Projects and Existing Scenarios

To understand the effect of the proposed project on survival, travel time, and routing of juvenile late-fall Chinook salmon, we simulated survival, travel time, and migration routing by using an 82-year time series of river flows and DCC gate operations under each scenario. Monthly river flows and DCC gate operations were simulated by using the CalSim II water-operations model and then disaggregated to daily river flows and gate operations for inputs into the Delta Simulation Model II (DSM2), a one-dimensional hydrodynamic model of the Delta. Because our model relied on measurements of daily inflows to the Delta and daily DCC-gate operations, we constructed the daily river flows and DCC-gate operations as inputs for DSM2 for input to the STARS model. The STARS model produced through-Delta survival rates, travel time, and migration routing distributions for a cohort of fish entering the Delta at Freeport on each day of the 82-year daily time series for each scenario.

The simulation output was summarized to provide useful statistics describing each daily cohort:

- The daily proportion of fish using each unique migration route.
- The daily proportion of fish entering the Interior Delta via the DCC and Georgiana Slough.
- Overall survival through the Delta, calculated as the mean survival rate of all individuals that entered the Delta on day *t*. Because routing for each individual was randomly drawn at each river junction, the mean survival is weighted by the proportion of fish that used each route.
- Median travel time over all routes for individuals that entered the Delta on day *t*. Median travel time was calculated by first adding reach-specific travel times for each individual between Freeport and Chipps Island and then calculating the exponent of the mean of the logarithms of the travel times.

To display model output, we generated four annual graphs:

- daily flows for each scenario,
- daily overall through-Delta survival ($S_{Delta}$) and median travel times,
- daily routing probabilities, and
- the median travel-time differences among scenarios in $S_{Delta}$, and the proportion of fish entering the Interior Delta.

For these graphs, we plotted the posterior medians and 80-percent credible intervals of the differences between scenarios. We presented data in the body of the report for two water years[1] to represent model output; graphs for all 82 years are provided in appendixes 1–8.

To summarize the 82-year time series, we used boxplots to examine the probabilities and magnitudes of differences in the daily survival rates, travel times between scenarios, and routing to the Interior Delta. For survival, we calculated the probability that survival for the PP or the PP2b was less than for the EX scenario. This probability was calculated as the fraction of the posterior distribution of the daily difference in survival between scenarios that was less than 0. For travel time and routing to the Interior Delta, we calculated the probability that travel time or routing for the PP or the PPb2 scenario was greater than under the EX scenario. This approach produced a daily time series of

[1] The 12-month period from October 1, for any given year, through September 30, of the following year. The water year is designated by the calendar year in which it ends.

probabilities for the 82-year simulation, which we summarized by using boxplots for each day of the year.

To examine the magnitudes of the differences in survival, travel time, or routing to the Interior Delta, we used boxplots to display the distributions of posterior median differences for all years combined and by water-year (WY) type. DWR uses five classifications for water-year type in the Sacramento Valley that are based on the water-year index value (WYI) in millions of acre-feet:

1. W=Wet, WYI greater than or equal to (≥)9.2;
2. AN=Above Normal, greater than or equal to 7.8 and less than (<)WYI≤9.2;
3. BN=Below Normal, 6.5≤WYI<7.8;
4. D=Dry, 5.4≤WYI<6.5; and
5. C=Critical, WYI<5.4 (Kapahi and others, 2006).

## Results and Discussion

We show detailed survival, travel time, and routing results of the PP and EX scenarios for two water years—WYs 1955, a dry water year, and 1990, a critically dry water year. We chose drier-than-normal years because these water-year types are more likely to lead to lower river flows, lower survival, and longer travel times. Results of the PP and EX scenarios for each of the 82-year time series are in Appendix 1. We show detailed single-year examples of only the PP and EX scenarios as the comparison between PP2b and EX scenarios are similar and found in Appendixes 5–8 (PP2b). We first focus on describing river flows and gate operations. For both water years, we noticed sharp monthly "steps" in simulated daily river discharge, which is different from actual river flows (figs. 5 and 6). The steps are also apparent in most other years (Appendix 1). The disaggregation from monthly to daily data involved using splines to transition from one month to the next to prevent model instabilities, thereby preserving the pattern of monthly steps in river flows (Steve Micko, Jacobs Engineering Group, written commun., May 9, 2019).

In WY 1955, 1990, and other water years (Appendix 1), we noticed differences in DCC gate operation between scenarios during the October–December period. Although both the PP and EX scenarios operate under the same DCC control rule, different flows for each scenario trigger DCC gate closures differently between scenarios. The number of gate-closure days each month between October 1 and December 14 was determined in CalSim II by using an empirical relationship between monthly average flow and the number of days per month that the flow at Wilkins Slough (USGS streamgage 11390500) exceeds 7,500 $ft^3/s$ (ICF International, 2016). Because the specific days of gate closure in each month are not specified by CalSim II, DSM2 inputs were structured under the assumption that gate openings occur on consecutive days in the beginning of each month, and closures occur at the end of each month (see figs. 5 and 6 as examples). For example, in 1955, lower Delta inflows at Freeport during October and November are likely associated with lower flows at Wilkins Slough, thereby triggering fewer gate-closure days and allowing the DCC to remain open longer under the PP scenario relative to the EX scenario (fig. 5).

For WY 1955, through-Delta survival under the PP scenario was considerably lower than the EX scenario during November owing to differences in discharge and operation of the DCC (fig. 5). During this period, the largest difference in survival (about 13 percentage points) occurred during early November, when the DCC was open during the PP but closed during the EX, and when discharge for PP was lower than for the EX. Patterns in travel time through the Delta were the opposite of patterns in survival, with longer median travel times under the PP scenario than the EX scenario during November (fig. 7). Owing to differences in both flow and DCC operation, a higher proportion of fish entered the Interior Delta through the Georgiana Slough and the DCC under the PP scenario than under the EX scenario (figs. 9 and 11). In contrast, for 1990, the critically dry year, discharge and DCC operation

were similar in October–December, leading to small differences in survival (fig. 6), travel time (fig. 8), or routing (figs. 10 and 12).

For WY 1955, differences in through-Delta survival between scenarios were caused by (1) the underlying flow-survival relationships, (2) differences in survival rates among routes, and (3) differences in routing that shifted fish between high- and low-survival routes. For example, under the PP scenario during October–November, simulations indicated that a high proportion of fish entered the DCC (fig. 9) relative to the EX scenario, which increased the proportion of fish experiencing low survival (fig. 4) and increased travel times (fig. 7). During October–November, flows under the PP scenario were lower than under the EX, which further increased the proportion of fish entering the Interior Delta (fig. 11), in turn exposing a higher fraction of fish to lower survival in the Interior Delta (fig. 3). Furthermore, an open DCC gate reduced flows in the Sacramento River downstream of the DCC and thus reduced survival of salmon that remained in the Sacramento River (Perry and others, 2018).

For both WY 1955 and 1990, survival was slightly higher under the PP scenario in April–June because of higher flows under the PP relative to EX (figs 5 and 6). During this period, higher flows reduced travel times (figs. 7 and 8) and slightly reduced entrainment into the Interior Delta (figs. 11 and 12). During the remainder of the year (January–April), there were essentially no differences in river flow or DCC gate operation, leading to no differences in survival, travel time, or routing (figs. 5–12). Detailed graphs for each water year, which are available in online appendixes, indicated seasonal patterns similar to those for WYs 1955 and 1990 (EX and PP scenarios appendixes 1–4, EX and PP2b scenarios appendixes 5–8).

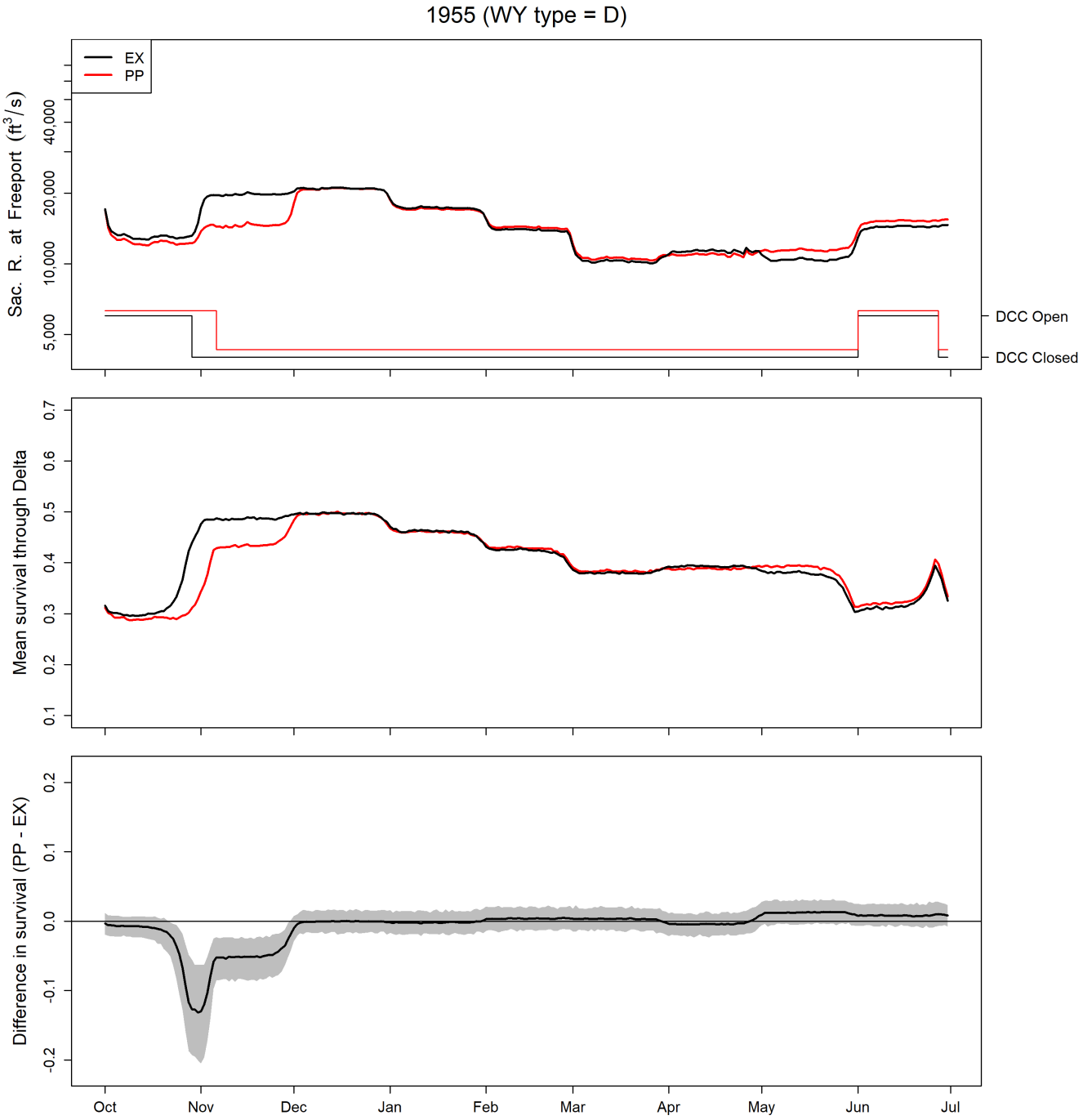


**Figure 5.** Graphs showing simulated daily bypass flows and Delta Cross Channel (DCC) gate operations for water year 1955 (top graph), medians of simulated mean daily survival through the Sacramento-San Joaquin River Delta, northern California (middle graph), and the differences in survival between the Proposed Project (PP) and Existing (EX) scenarios (bottom graph). Heavy lines in the top graph show discharge of the Sacramento River (Sac. R.) at Freeport on the primary y-axis, and thin lines show DCC operation (gate open or closed) on the second y-axis. Discharge in the top graph is shown on a logarithmic scale to highlight the variation in low discharge values. In the bottom graph, the gray-shaded region shows the 90-percent credible interval on the difference in survival between scenarios. D, Dry; WY, water year; $ft^3/s$, cubic foot per second.

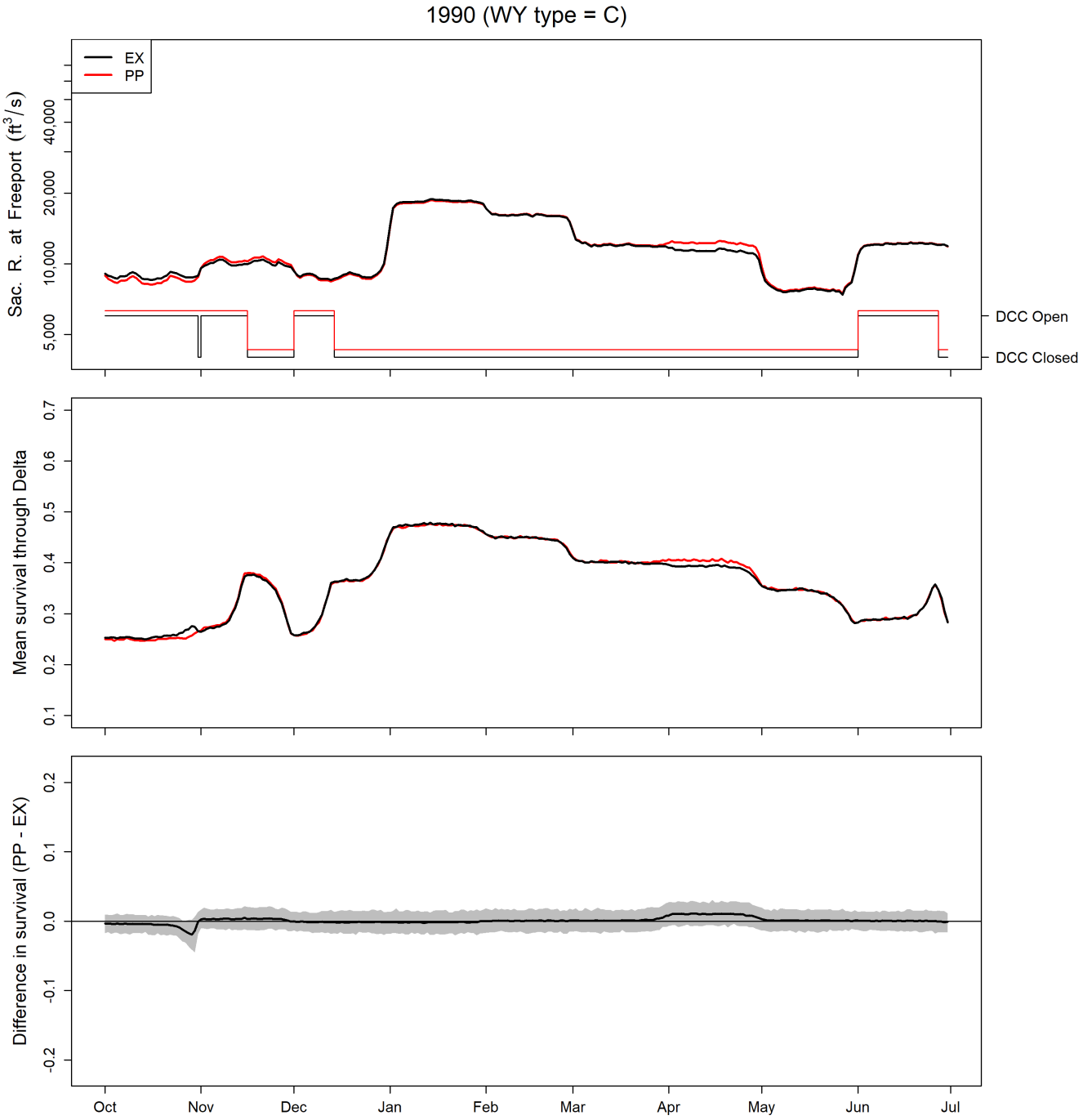


**Figure 6.** Graphs showing simulated daily bypass flows and Delta Cross Channel (DCC) gate operations for water year 1990 (top graph), median of simulated mean daily survival through the Sacramento-San Joaquin River Delta, northern California (middle graph), and the difference in survival between the Proposed Project (PP) and Existing (EX) scenarios (bottom graph). Heavy lines in the top graph shows discharge of the Sacramento River (Sac. R.) at Freeport on the primary y-axis, and thin lines show DCC operation (gate open or closed) on the second y-axis. Discharge in the top graph is shown on a logarithmic scale to highlight variation in low discharge values. In the bottom graph, the gray-shaded region shows the 90-percent credible interval of the difference in survival rates between scenarios. C, Critical; WY, water year; $ft^3/s$, cubic foot per second.

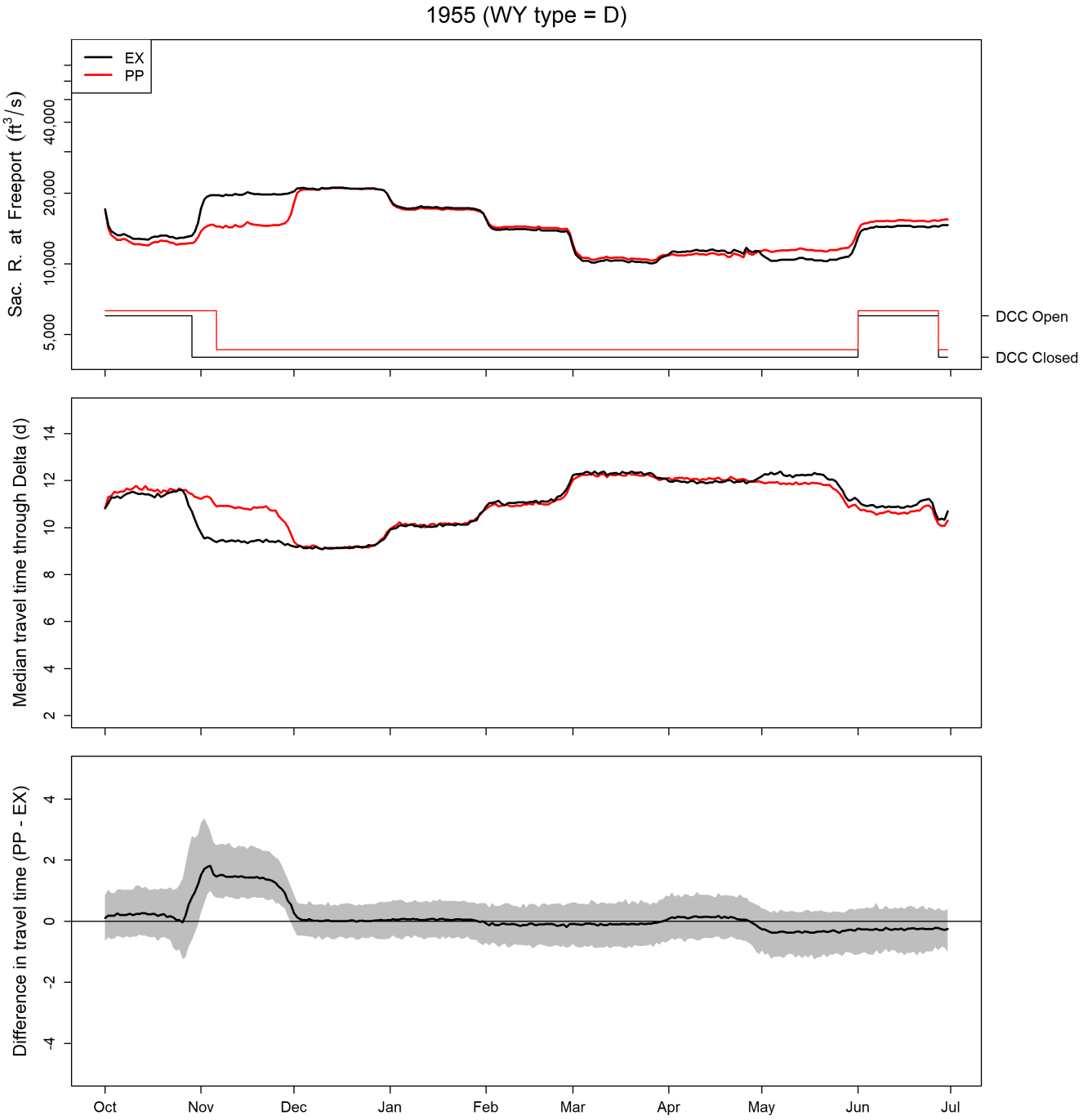


**Figure 7.** Graphs showing simulated daily bypass flows and Delta Cross Channel (DCC) gate operations for water year 1955 (top graph), simulated median daily travel time of juvenile Chinook salmon through the Sacramento-San Joaquin River Delta, northern California (middle graph), and the difference in travel time between the Proposed Project (PP) and Existing (EX) scenarios (bottom graph). Heavy lines in the top graph show discharge of the Sacramento River (Sac. R.) at Freeport on the primary y-axis, and thin lines show DCC operation (gate open or closed) on the second y-axis. Discharge in the top graph is shown on a logarithmic scale to highlight variation in low discharge values. In the bottom graph, the gray-shaded region shows the 90-percent credible interval of the difference in median travel times between scenarios. D, Dry; WY, water year; $ft^3/s$, cubic foot per second.

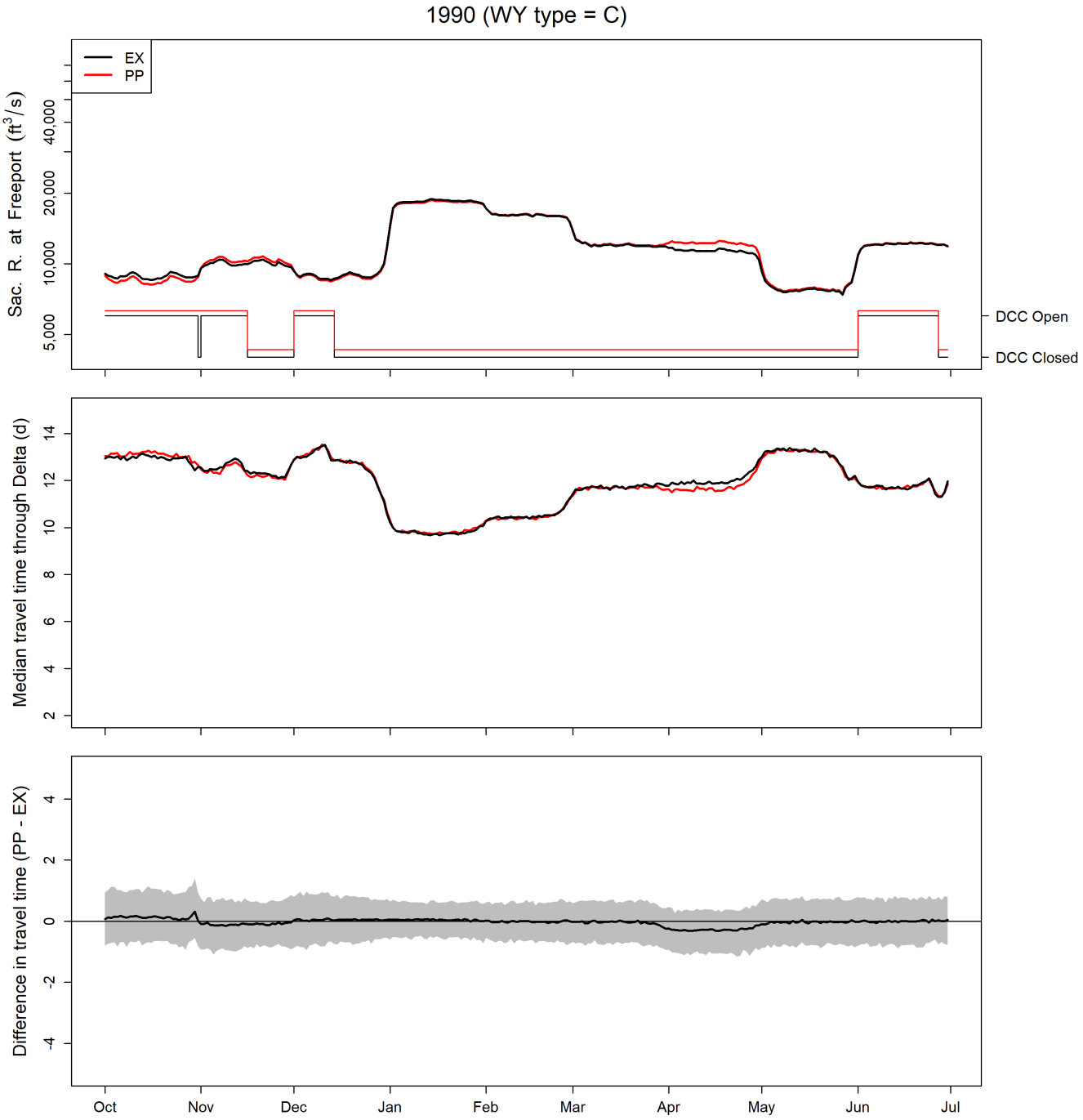


**Figure 8.** Graphs showing simulated daily bypass flows and Delta Cross Channel (DCC) gate operations for water year 1990 (top graph), simulated median daily travel time of juvenile Chinook salmon through the Sacramento-San Joaquin River Delta, northern California (middle graph), and the difference in travel time between the Proposed Project (PP) and Existing (EX) scenarios (bottom graph). Heavy lines in the top graph show discharge of the Sacramento River (Sac. R.) at Freeport on the primary y-axis, and thin lines show DCC operation (gate open or closed) on the second y-axis. Discharge in the top graph is shown on a logarithmic scale to highlight variation in low discharge values. In the bottom graph, the gray-shaded region shows the 90-percent credible interval of the difference in median travel time between scenarios. C, Critical; WY, water year; $ft^3/s$, cubic foot per second.

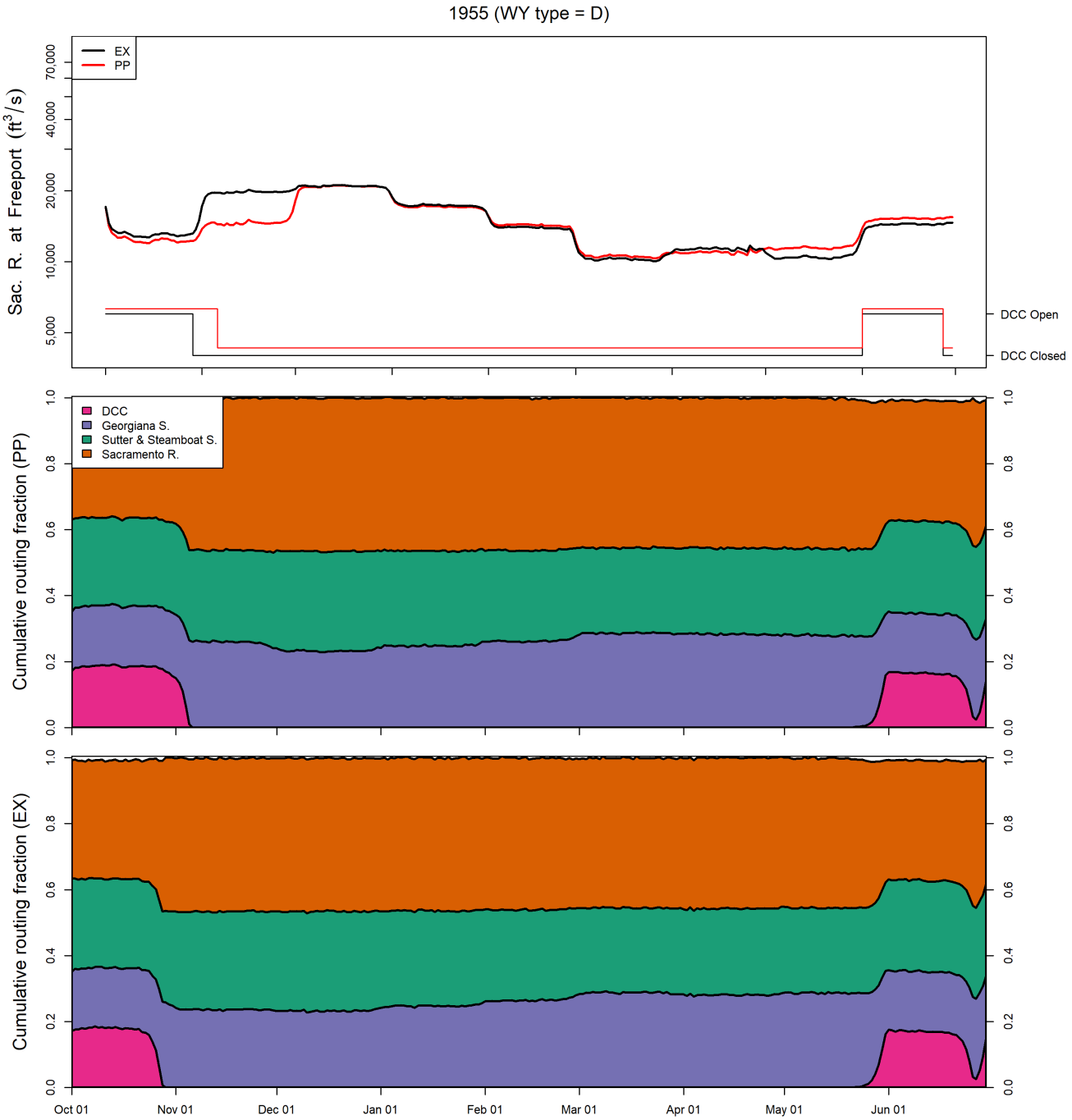


**Figure 9.** Graphs showing simulated daily bypass flows and Delta Cross Channel (DCC) gate operations for water year 1955 (top graph), and stacked line plots showing the daily cumulative migration-route probabilities for the Proposed Project (PP, middle graph) and Existing (EX, bottom graph) scenarios, Sacramento-San Joaquin River Delta, northern California. Heavy lines in the top graph show discharge of the Sacramento River (Sac. R.) at Freeport on the primary y-axis, and thin lines show DCC operation (gate open or closed) on the second y-axis. Discharge in the top graph is shown on a logarithmic scale to highlight variation in low discharge values. D, Dry; WY, water year; $ft^3/s$, cubic foot per second.

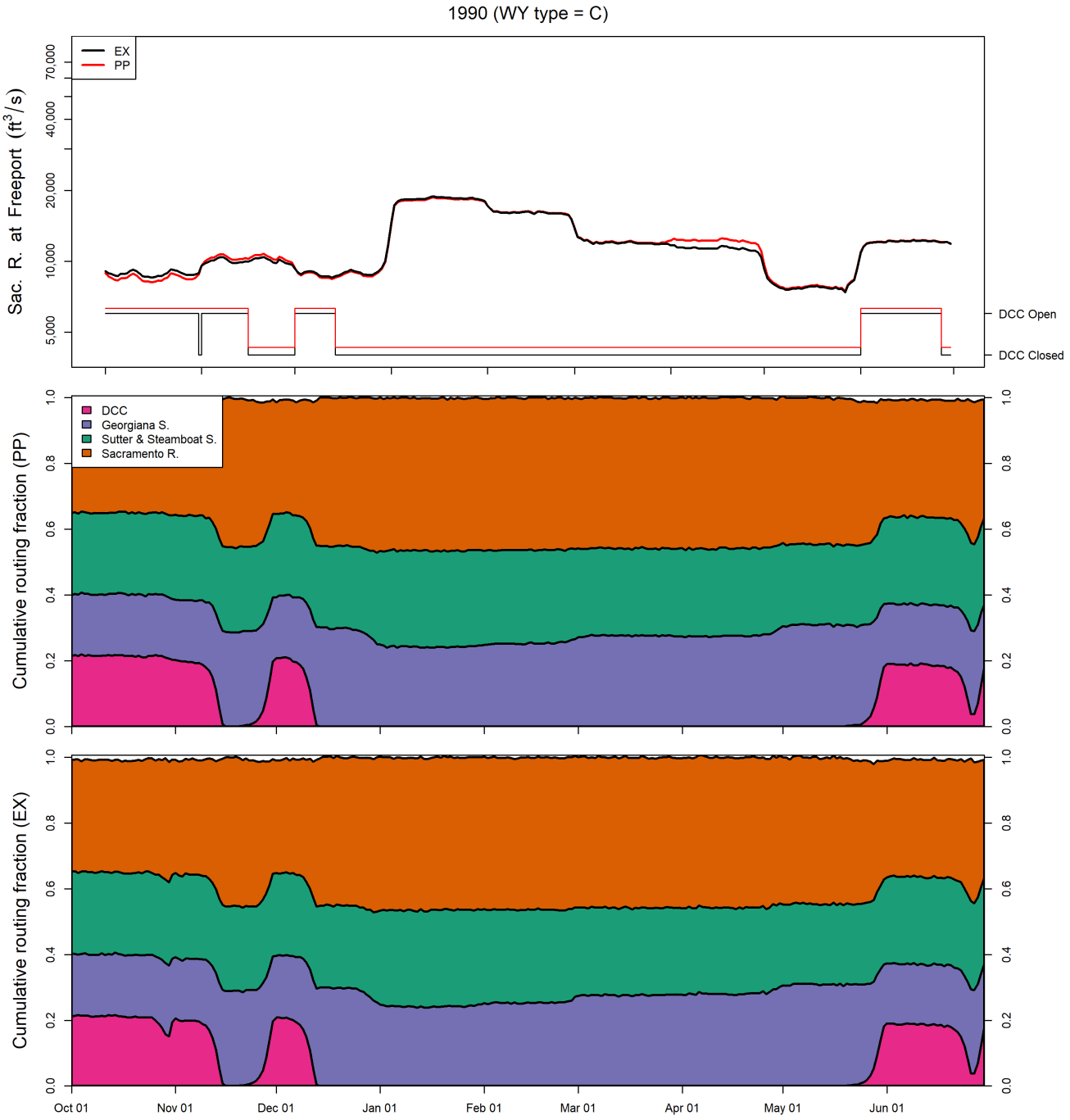


**Figure 10.** Graphs showing simulated daily bypass flows and Delta Cross Channel (DCC) gate operations for water year 1990 (top graph), and stacked line plots showing the daily cumulative migration-route probabilities for the Proposed Project (PP, middle graph) and Existing (EX, bottom graph) scenarios, Sacramento-San Joaquin River Delta, northern California. Heavy lines in the top graph show discharge of the Sacramento River (Sac. R.) at Freeport on the primary y-axis, and thin lines show DCC operation (gate open or closed) on the second y-axis. Discharge in the top graph is shown on a logarithmic scale to highlight variation in low discharge values. C, Critical; WY, water year; $ft^3/s$, cubic foot per second.

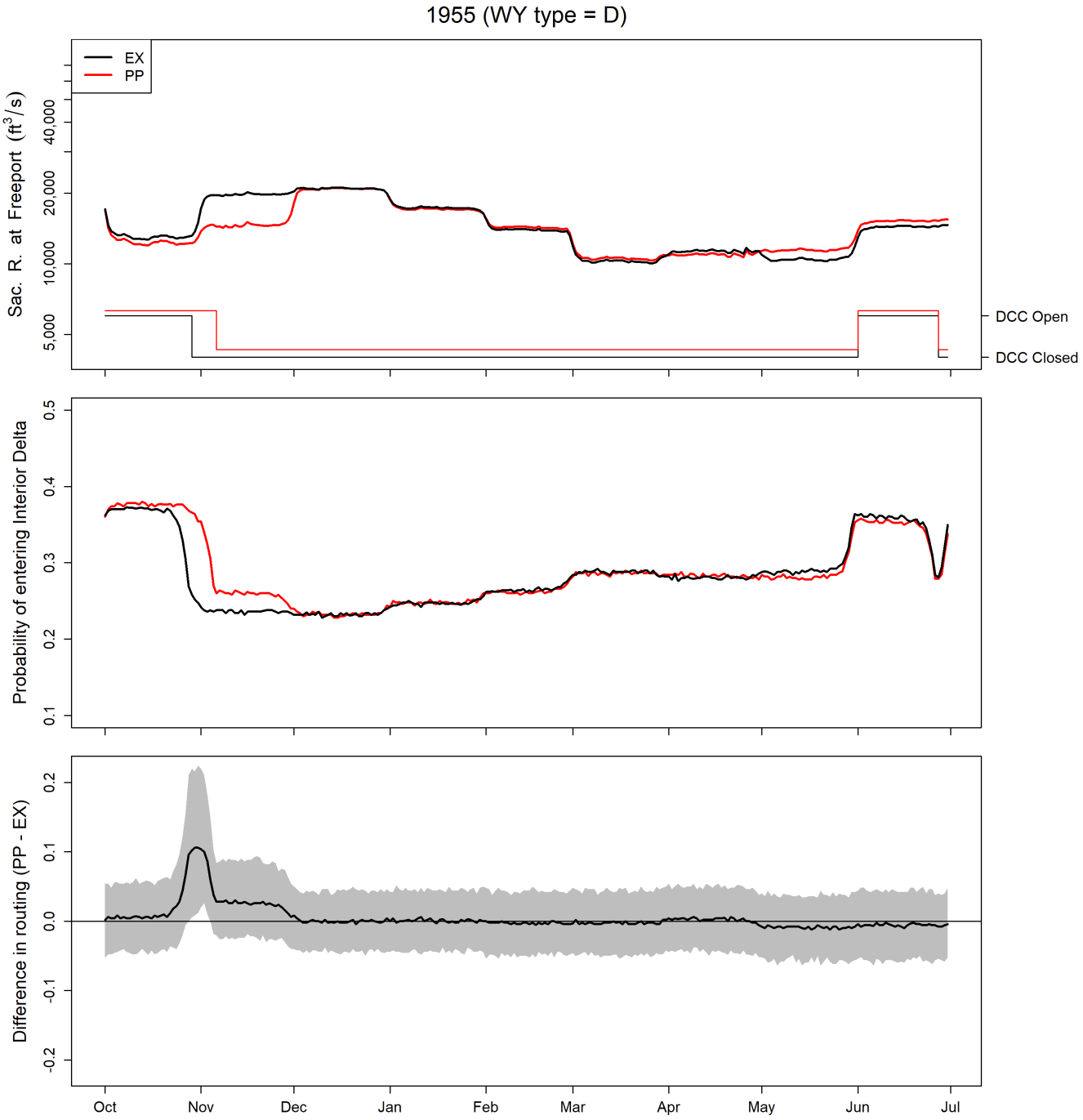


**Figure 11.** Graphs showing simulated daily bypass flows and Delta Cross Channel (DCC) gate operations for water year 1955 (top graph), simulated median probability of entering the Interior Delta through the Delta Cross Channel or Georgiana Slough (middle graph), and the difference in routing between the Proposed Project (PP) and Existing (EX) scenarios (bottom graph). Heavy lines in the top graph show discharge of the Sacramento River (Sac. R.) at Freeport on the primary y-axis, and thin lines show DCC operation (gate open or closed) on the second y-axis. Discharge in the top graph is shown on a logarithmic scale to highlight variation in low discharge values. In the bottom graph, the gray-shaded region shows the 90-percent credible interval of the difference in routing between scenarios. D, Dry; WY, water year; $ft^3/s$, cubic foot per second.

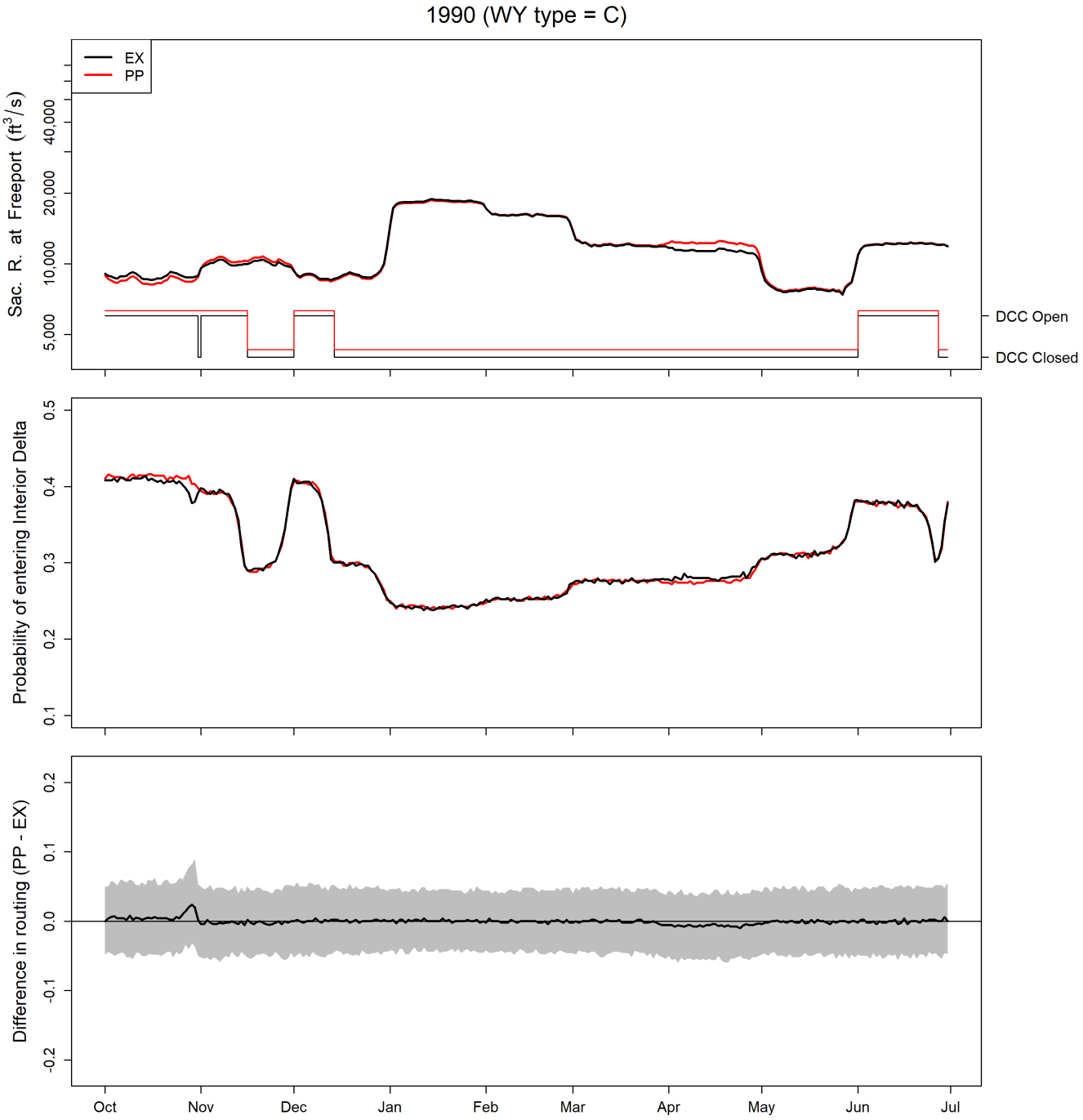


**Figure 12.** Graphs showing simulated daily bypass flows and Delta Cross Channel (DCC) gate operations for water year 1990 (top graph), simulated median probability of entering the Interior Delta through the Delta Cross Channel or Georgiana Slough (middle graph), and the difference in routing between the Proposed Project (PP) and Existing (EX) scenarios (bottom graph). Heavy lines in the top graph show discharge of the Sacramento River (Sac. R.) at Freeport on the primary y-axis, and thin lines show DCC operation (gate open or closed) on the second y-axis. Discharge in the top graph is shown on a logarithmic scale to highlight variation in low discharge values. In the bottom graph, the gray-shaded region shows the 90-percent credible interval of the difference in routing between scenarios. C, Critical; WY, water year; $ft^3/s$, cubic foot per second.

## Proposed Project

Summaries of the 82-year simulation indicated consistent seasonal patterns between the EX and the first proposed project (PP) scenarios, reflecting seasonal differences in operation under each scenario. The simulations indicated a median probability of 0.5 that survival for the PP scenario was less than that for the EX scenario throughout the year (fig. 13). In November, the 25th percentile was about 0.5, indicating that 25 percent of the years had a 50-percent probability or greater that survival under the PP was less than under the EX. In November, the 75th percentile was about one, indicating that 75 percent of water years had a 100-percent probability or less that survival under PP was less than under the EX. Similar patterns are visible in probability plots of travel time (fig. 14) and routing (fig. 15) during this period. In October and December, the 25th percentile of through-Delta survival was about 0.2, and the 75th percentile was about 0.6, while the median was near 0.5. Similarly, the patterns in May and June were the same but at a smaller scale, with the May 25th percentile at about 0.3 and the May 75th percentile at about 0.5. In February–April, the 75th percentile of through-Delta survival was about 0.5, and the 25th percentile was about 0.4. Similar patterns occurred with travel time (fig. 14) and routing (fig. 15) during this period.

Boxplots of the median differences between scenarios revealed seasonal patterns in the magnitudes of the differences in survival, travel time, and migration routing. During November, the median of the survival difference between the PP and EX was about -0.01 (fig. 16). Although the median difference was small, the 25th percentile approached -0.10 in mid-November, indicating that survival under the PP scenario was more than 10 percentage points lower than under the EX scenario in 25 percent of water years. Similar patterns occurred with median travel time (fig. 17) and routing into the Interior Delta (fig. 18), except in the opposite direction of survival. For October, December, May, and June, the 25th and 75th percentiles of survival differences between scenarios were a few percent above zero, indicating that a small increase in survival under the PP was higher than under the EX in 25–75 percent of years (fig. 16). Travel time (fig. 17) and routing to the Interior Delta (fig. 18) showed patterns similar to those for October, December, May, and June, but in the opposite direction of survival.

Differences in survival (fig. 19), travel time (fig. 20), and routing (fig. 21) between scenarios varied among water year types and seasons. In October–December, survival differences were similar among water-year types but with decreasing magnitude as the water year ranges from wet to critically dry. In contrast, in January, differences in survival between scenarios were lower in critically dry compared to wet and dry years, in which differences were again lower than during above-normal and below-normal years (fig. 19). Survival differences in October, December, May, and June were greater in above-normal, below-normal, and dry years compared to wet and critical, but with less magnitude. Similar patterns among water-year types were evident for travel time (fig. 20) and routing to the Interior Delta (fig. 21).

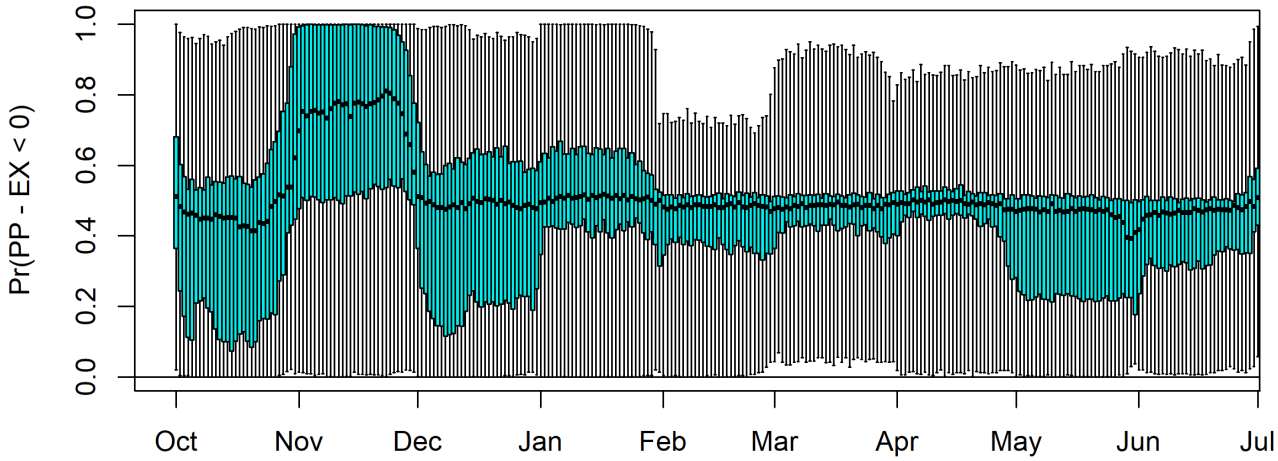


**Figure 13.** Boxplots showing the distribution of the probability that through-Delta survival for the Proposed Project (PP) scenario is less than survival for the Existing (EX) scenario. Each boxplot represents the distribution among the 82 years for a given date of the probability that the difference between PP and EX is less than zero. The point in each box represents the median, the box hinges bounding the shaded blue area represent the 25th and 75th percentiles, and the whiskers display the minimum and maximum. Pr, probability; <, less than.

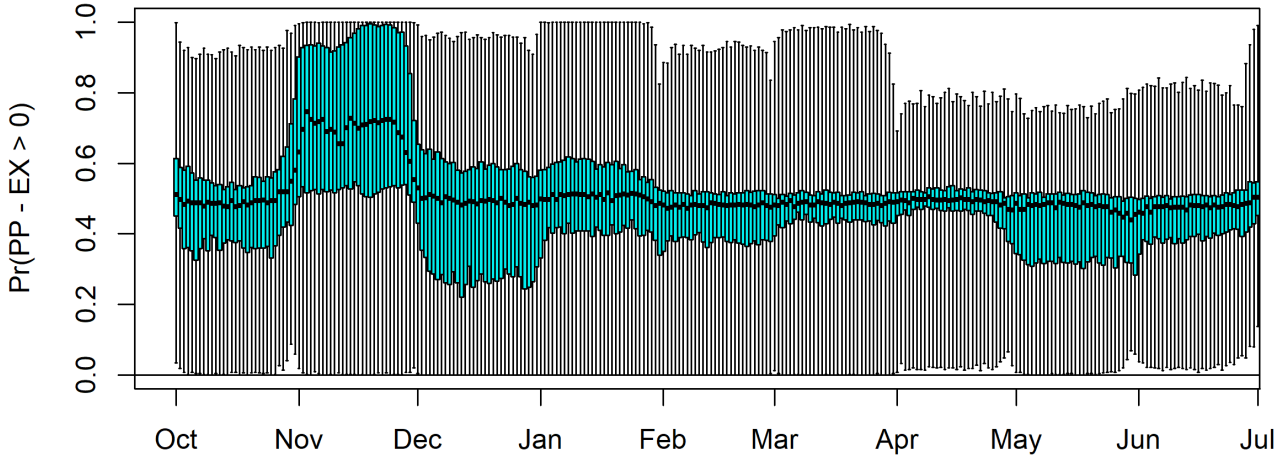


**Figure 14.** Boxplots showing the distribution of the probability that the difference in median travel times through the Delta between the Existing (EX) and Proposed Project (PP) scenarios is greater than zero. Each boxplot represents the distribution among the 82 years for a given date of the probability that the difference between PP and EX is greater than zero. The point in each box represents the median, the box hinges bounding the shaded blue area represent the 25th and 75th percentiles, and the whiskers display the minimum and maximum. Pr, probability; >, greater than.

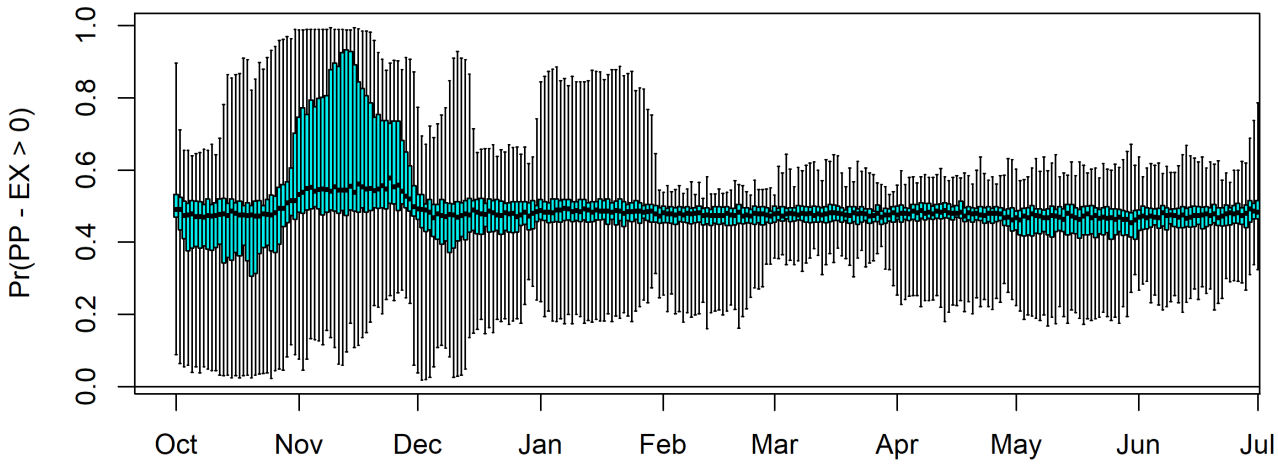


**Figure 15.** Boxplots showing the distribution of the probability that the difference in being routed into the Interior Delta between the Existing (EX) and Proposed Project (PP) scenarios is greater than zero. Each boxplot represents the distribution among the 82 years for a given date of the probability that the difference between PP and EX is greater than zero. The point in each box represents the median, the box hinges bounding the shaded blue area represent the 25th and 75th percentiles, and the whiskers display the minimum and maximum. Pr, probability; >, greater than.

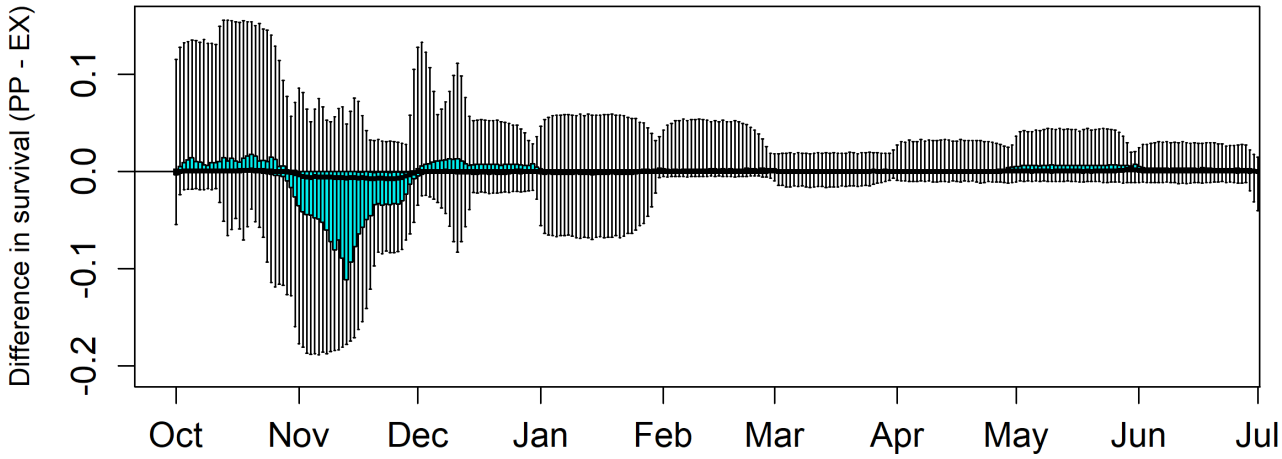


**Figure 16.** Boxplots of daily median differences in through-Delta survival between the Proposed Project (PP) and Existing (EX) scenarios. Each boxplot represents the distribution of median survival differences among the 82 years for a given date. The point in each box represents the median, the box hinges bounding the shaded blue area represent the 25th and 75th percentiles, and the whiskers display the minimum and maximum.

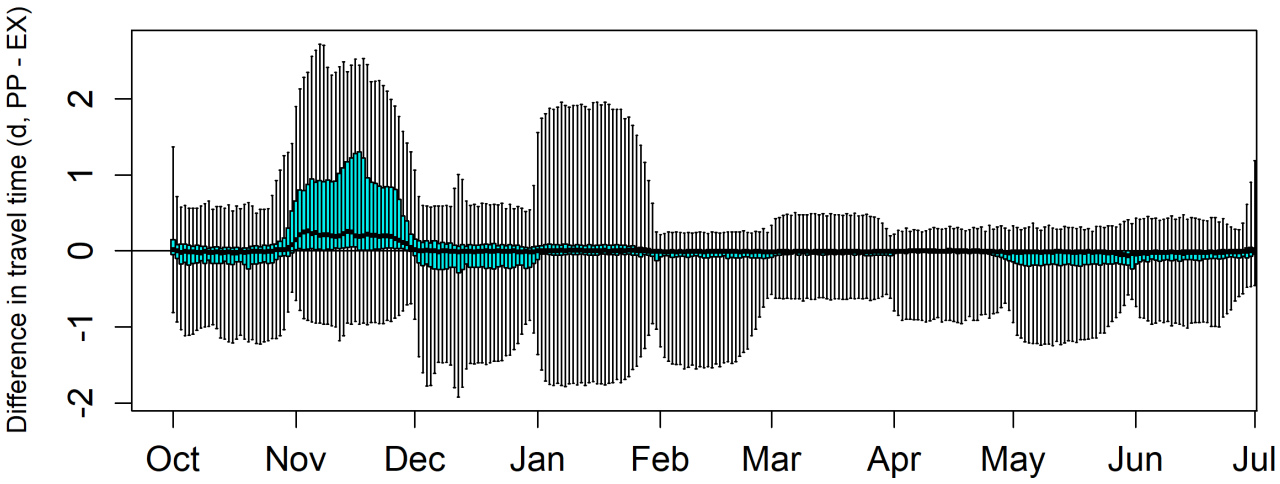


**Figure 17.** Daily boxplots of differences in median travel times between the Proposed Project (PP) and Existing (EX) scenarios. Each boxplot represents the distribution of median travel-time differences among the 82 years for a given date. The point in each box represents the median, the box hinges bounding the shaded blue area represent the 25th and 75th percentiles, and the whiskers display the minimum and maximum. d, days.

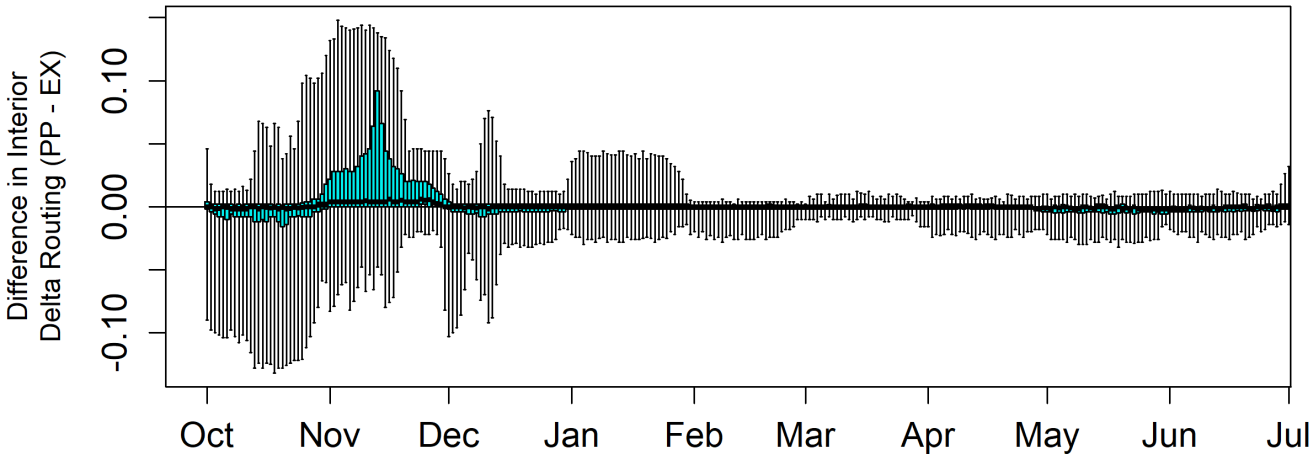


**Figure 18.** Daily boxplots of differences in routing to the Interior Delta between the Proposed Project (PP) and Existing (EX) scenarios. Each boxplot represents the distribution of median routing differences among the 82 years for a given date. The point in each box represents the median, the box hinges bounding the shaded blue area represent the 25th and 75th percentiles, and the whiskers display the minimum and maximum.

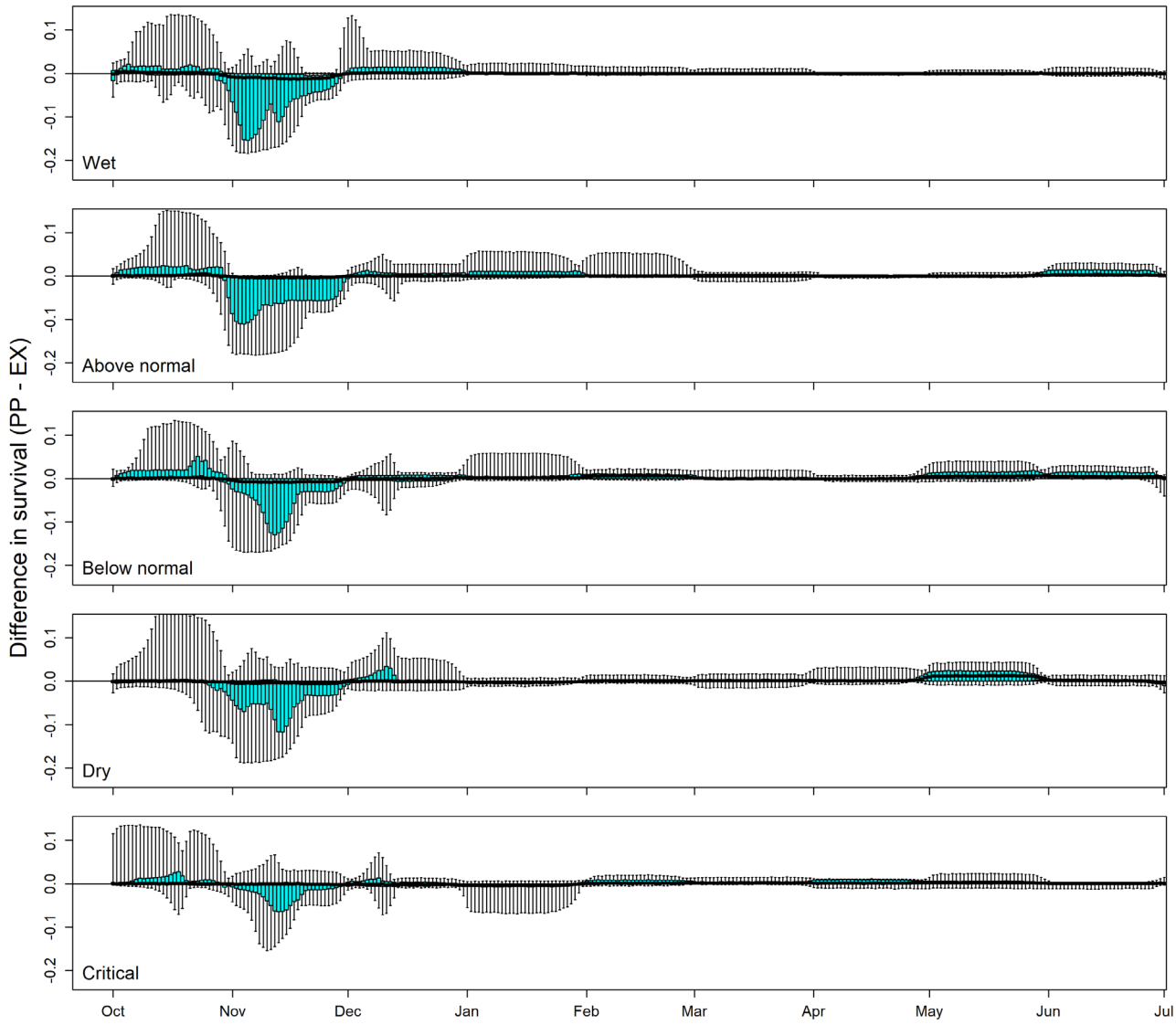


**Figure 19.** Daily boxplots of median differences in through-Delta survival rates between the Proposed Project (PP) and Existing (EX) scenarios by water-year type. Each boxplot represents the distribution of median survival differences among the 82 years for a given date. The point in each box represents the median, the box hinges bounding the shaded blue area represent the 25th and 75th percentiles, and the whiskers display the minimum and maximum.

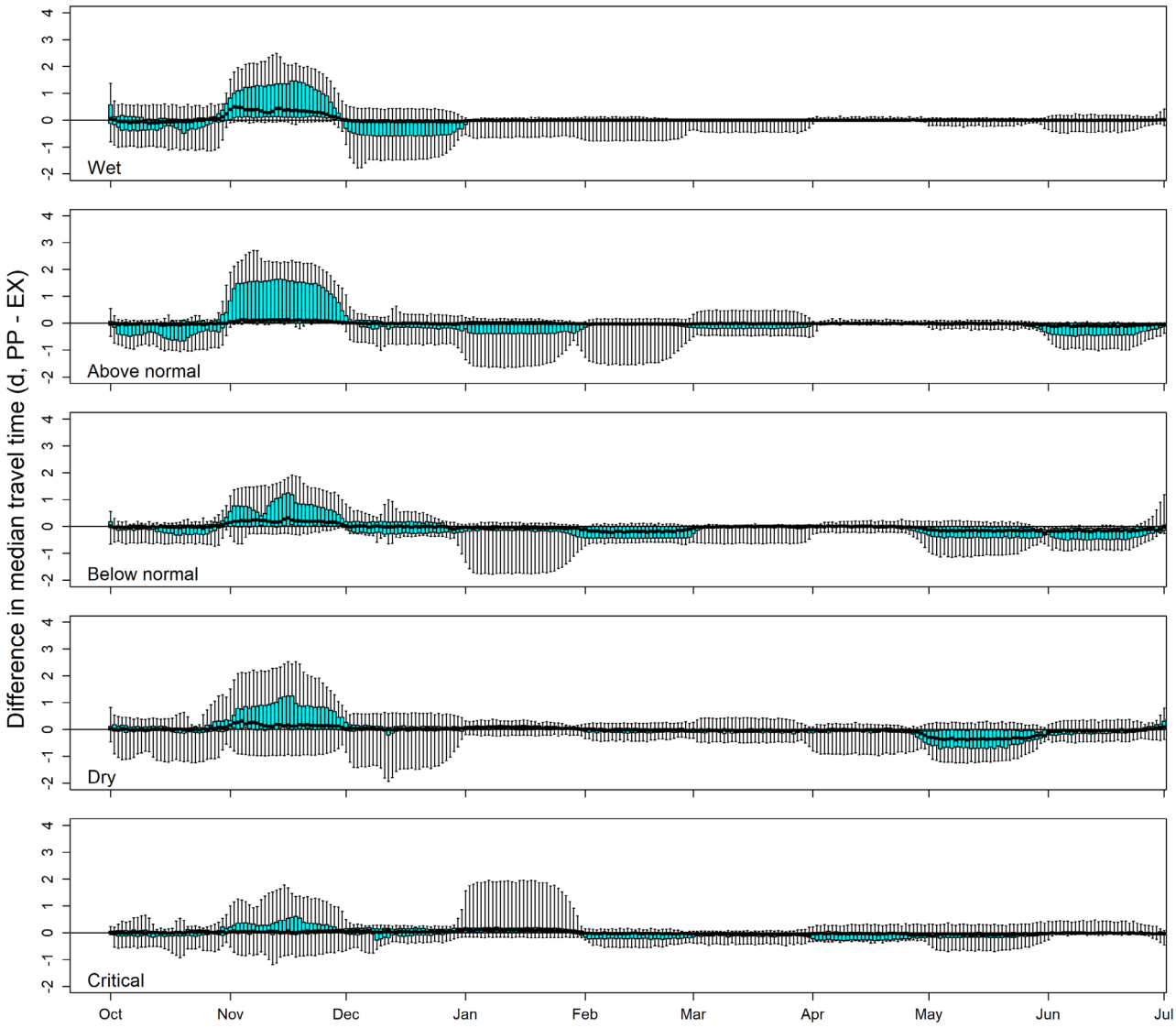


**Figure 20.** Daily boxplots of median differences in median travel time between the Proposed Project (PP) and Existing (EX) scenarios by water-year type. Each boxplot represents the distribution of median travel-time differences among the 82 years for a given date. The point in each box represents the median, the box hinges bounding the shaded blue area represent the 25$^{th}$ and 75th percentiles, and the whiskers display the minimum and maximum. d, days.

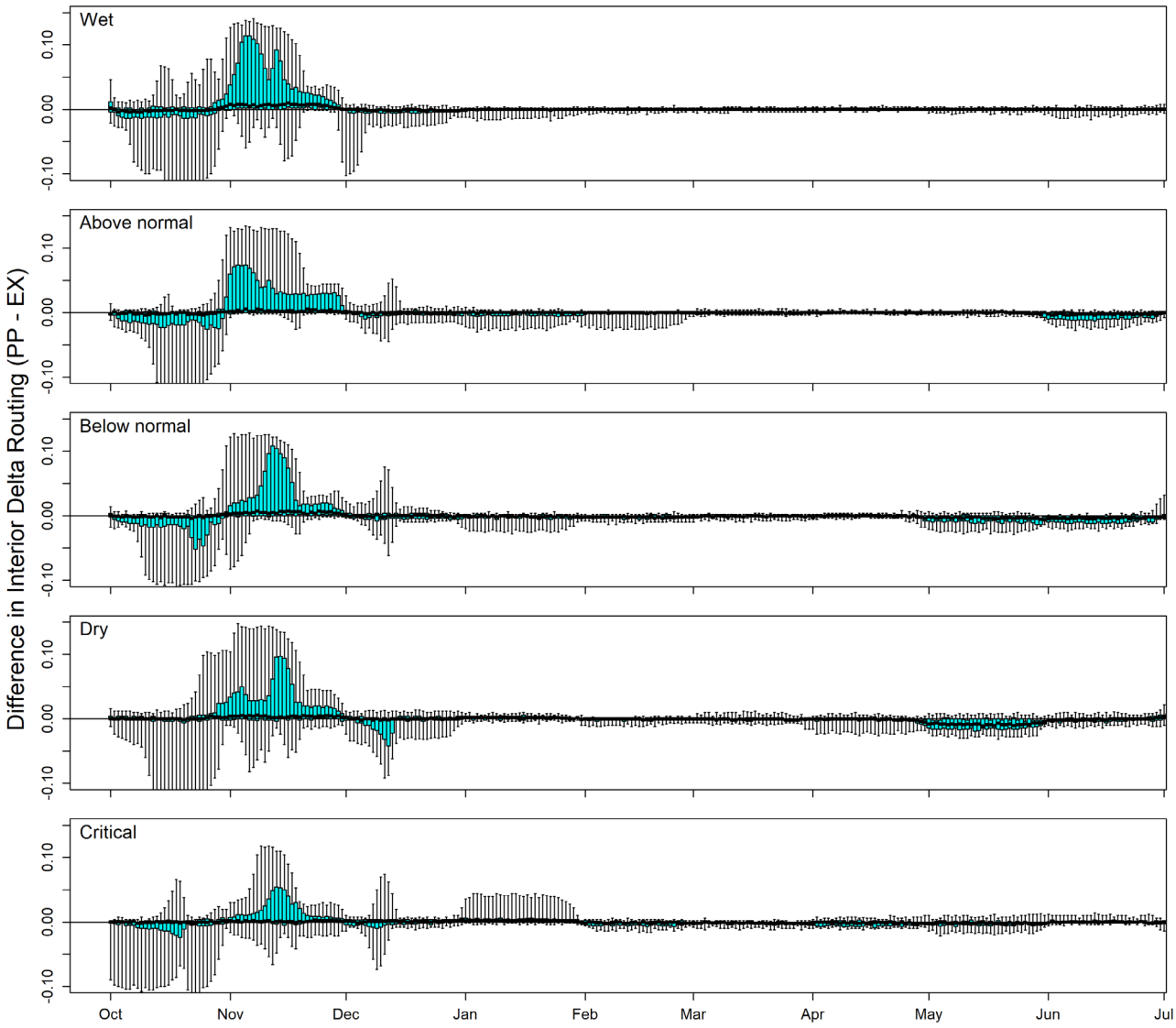


**Figure 21.** Daily boxplots of median differences in routing to the Interior Delta between the Proposed Project (PP) and Existing (EX) scenarios by water-year type. Each boxplot represents the distribution of median travel-time differences among 82 years for a given date. The point in each box represents the median, the box hinges bounding the shaded blue area represent the 25th and 75th percentiles, and the whiskers display the minimum and maximum.

## Proposed Project 2b

Summaries of the 82-year simulation indicated consistent seasonal patterns between the EX and the second proposed project (PP2b) scenarios, reflecting seasonal differences in operation under each scenario. The simulations indicated a median probability of 0.5 that survival for the PP2b scenario was less than for the EX scenario throughout all months of the year except November (fig. 22). In November, the 25th percentile was about 0.5, indicating that 25 percent of the years had a 50-percent probability or greater that survival under the PP2b was less than under the EX. The 75th percentile in November was about 1.0, indicating that 75 percent of water years had a 100 percent probability or less that survival under the PP2b was less than under the EX and the median was about

0.8. In October and December, the 25th percentile of through-Delta survival was between about 0.2 and 0.3, the 75th percentile was about 0.7, and the median was about 0.5. During May and June, the 25th percentile was between about 0.2 and 0.3, while the 75th percentile was just over 0.5. In February–April, the 75th percentile of through-Delta survival was about 0.5, and the 25th percentile was less than 0.4. Similar patterns occurred with travel time (fig. 23) and routing (fig. 24) during these periods.

Boxplots of the median differences between the EX and PP2b scenarios revealed seasonal patterns in the magnitudes of the differences in survival, travel time, and migration routing. During November, the median of the survival difference between the PP2b and EX scenarios was just less than 0 (fig. 25). Although the median difference was small, the 25th percentile approached -0.10 in mid-November, indicating that survival under the PP2b scenario was more than 10 percentage points lower than under the EX scenario in 25 percent of water years. Similar patterns occurred with median travel time (fig. 26) and routing into the Interior Delta (fig. 27), except in the opposite direction of survival. In October, December, and May, the 75th percentile was just over 1.0 indicating that survival during the PP2b scenario was higher than during the EX scenario in 75 percent of the years. Travel time (fig. 26) and routing to the Interior Delta (fig. 27) showed patterns similar to those for October, December, and May, but in the opposite direction of survival.

Differences in survival (fig. 28), travel time (fig. 29), and routing (fig. 30) between scenarios varied among water year types and seasons. In all water year types, through-Delta survival was lower in November during the PP2b scenario compared to the EX scenario (fig. 28). The magnitude of the November difference was largest in wet water years and smallest in the critically dry water years. In October for all water year types, through-Delta survival was higher during the PP2b scenario compared to the EX scenario. The 75th percentile of through-Delta survival was higher during the PP2b scenario compared to the EX scenario in above normal water years during January and June; in December, January, May, and June in below normal water years; during December, May, and June in dry water years; and during December in wet and critically dry years. Similar patterns among water-year types were evident for travel time (fig. 29) and routing to the Interior Delta (fig. 30).

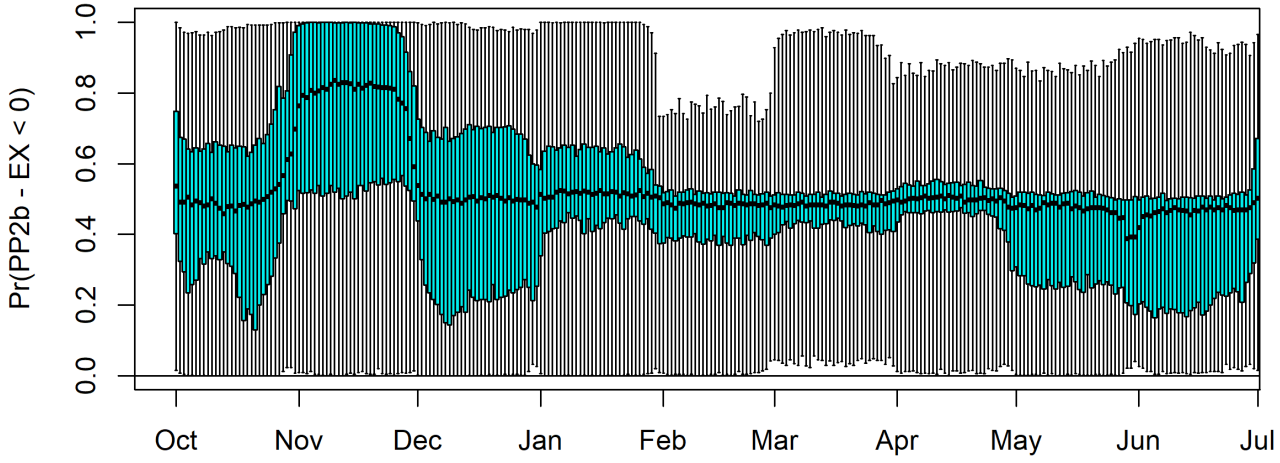


**Figure 22.** Boxplots showing the distribution of the probability that through-Delta survival for the Proposed Project 2b (PP2b) scenario is less than survival for the Existing (EX) scenario. Each boxplot represents the distribution among the 82 years for a given date of the probability that the difference between PP2b and EX is less than zero. The point in each box represents the median, the box hinges bounding the shaded blue area represent the 25th and 75th percentiles, and the whiskers display the minimum and maximum. Pr, probability; <, less than.

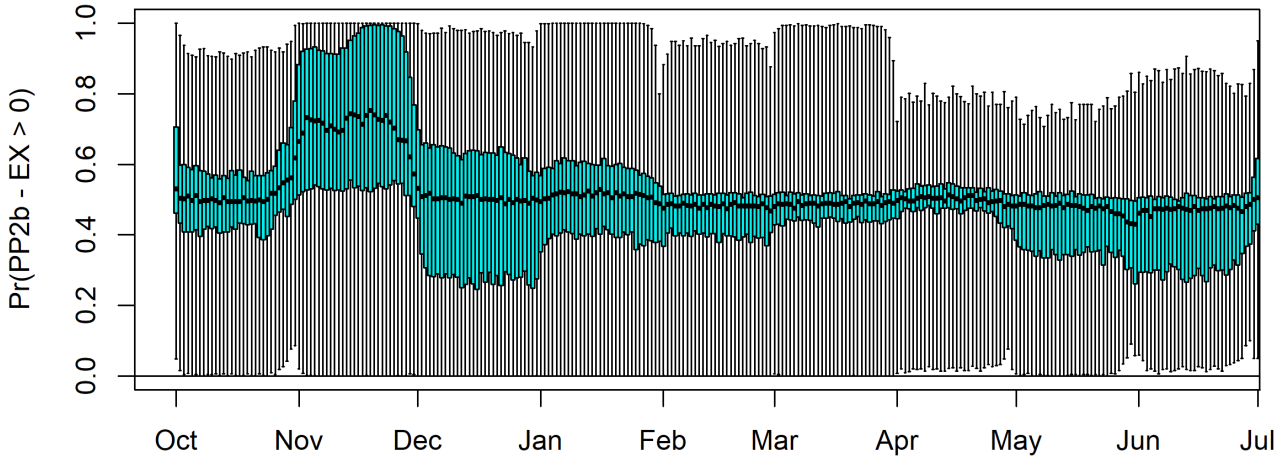


**Figure 23.** Boxplots showing the distribution of the probability that the difference in median travel times through the Delta between the Existing (EX) and Proposed Project 2b (PP2b) scenarios is greater than zero. Each boxplot represents the distribution among the 82 years for a given date of the probability that the difference between PP2b and EX is greater than zero. The point in each box represents the median, the box hinges bounding the shaded blue area represent the 25th and 75th percentiles, and the whiskers display the minimum and maximum. Pr, probability; >, greater than.

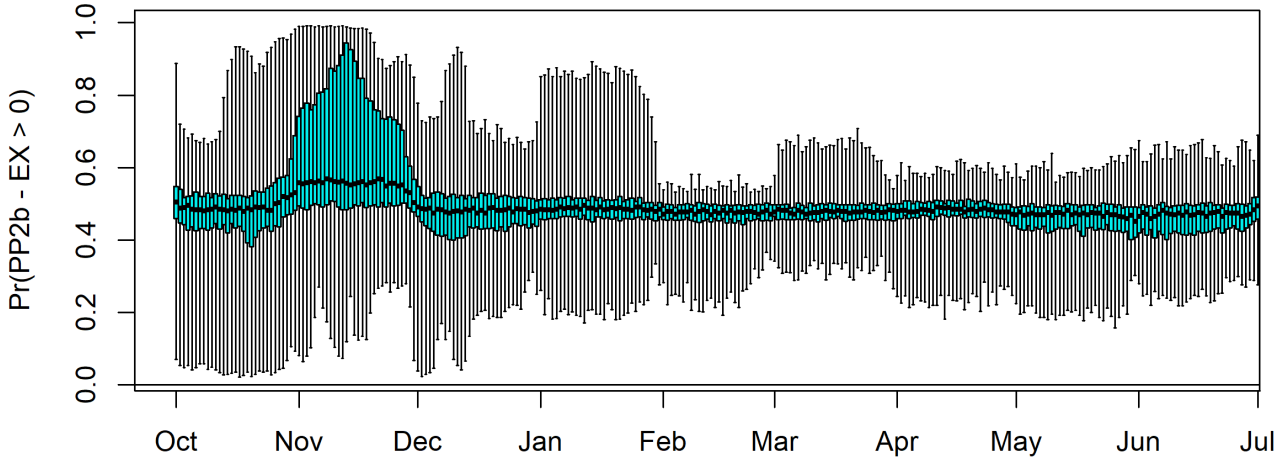


**Figure 24.** Boxplots showing the distribution of the probability that the difference in being routed into the Interior Delta between the Existing (EX) and Proposed Project 2b (PP2b) scenarios is greater than zero. Each boxplot represents the distribution among the 82 years for a given date of the probability that the difference between PP2b and EX is greater than zero. The point in each box represents the median, the box hinges bounding the shaded blue area represent the 25th and 75th percentiles, and the whiskers display the minimum and maximum. Pr, probability; >, greater than.

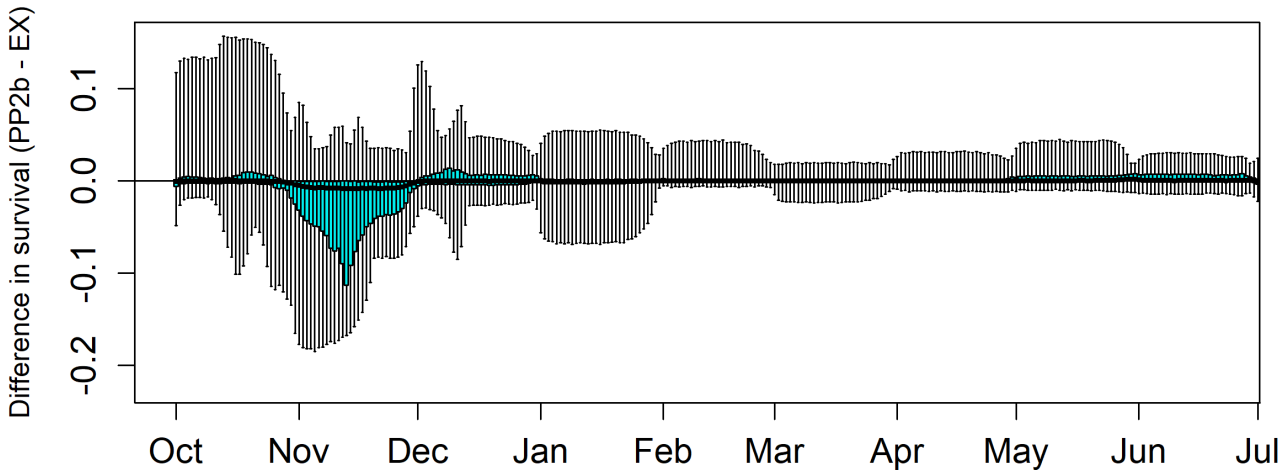


**Figure 25.** Boxplots of daily median differences in through-Delta survival between the Proposed Project 2b (PP2b) and Existing (EX) scenarios. Each boxplot represents the distribution of median survival differences among the 82 years for a given date. The point in each box represents the median, the box hinges bounding the shaded blue area represent the 25th and 75th percentiles, and the whiskers display the minimum and maximum.

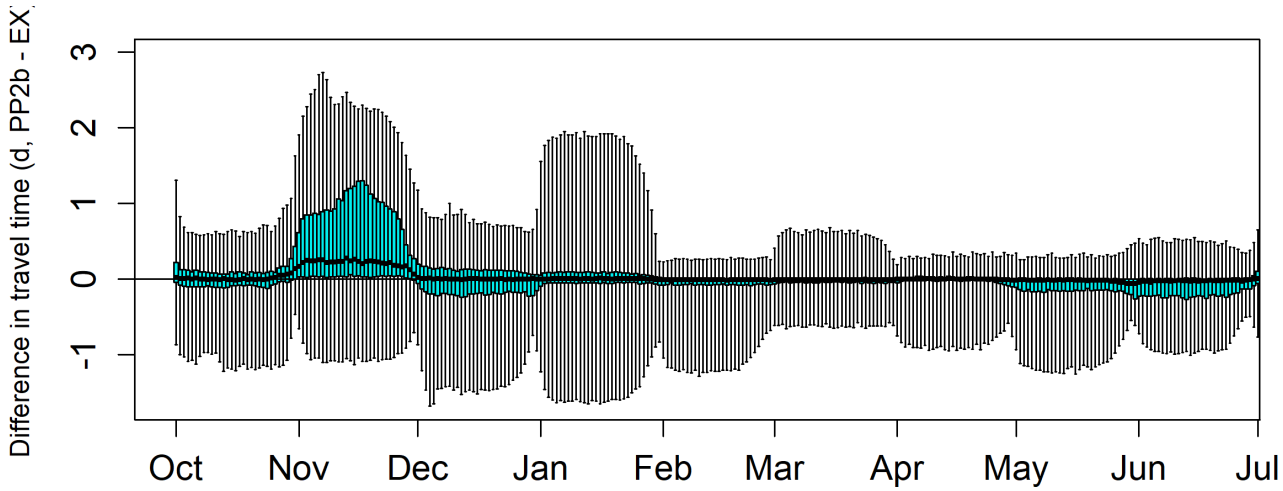


**Figure 26.** Daily boxplots of differences in median travel times between the Proposed Project 2b (PP2b) and Existing (EX) scenarios. Each boxplot represents the distribution of median travel-time differences among the 82 years for a given date. The point in each box represents the median, the box hinges bounding the shaded blue area represent the 25th and 75th percentiles, and the whiskers display the minimum and maximum. d, days.

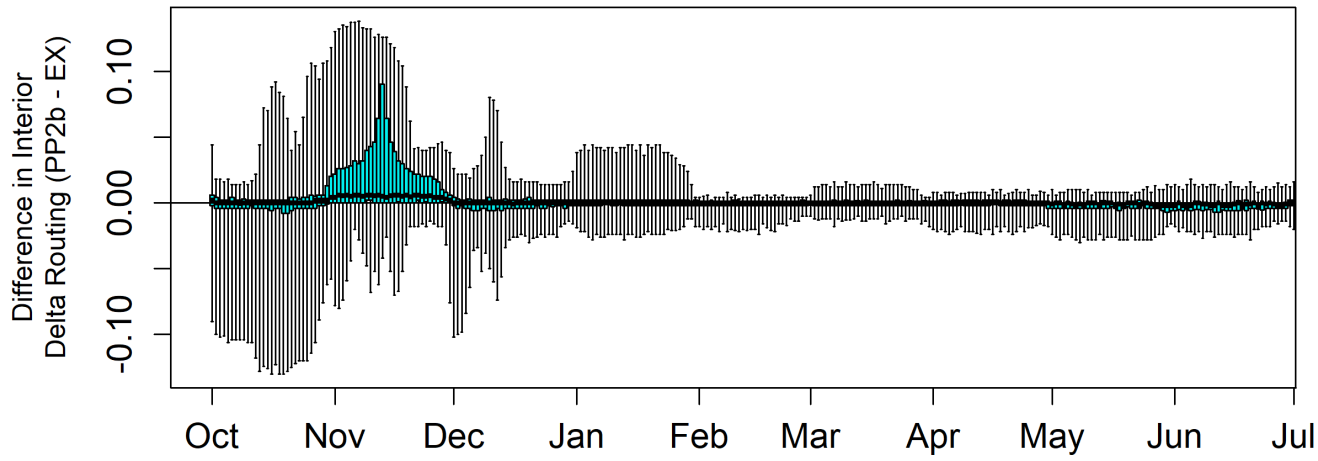


**Figure 27.** Daily boxplots of differences in routing to the Interior Delta between the Proposed Project 2b (PP2b) and Existing (EX) scenarios. Each boxplot represents the distribution of median routing differences among the 82 years for a given date. The point in each box represents the median, the box hinges bounding the shaded blue area represent the 25th and 75th percentiles, and the whiskers display the minimum and maximum.

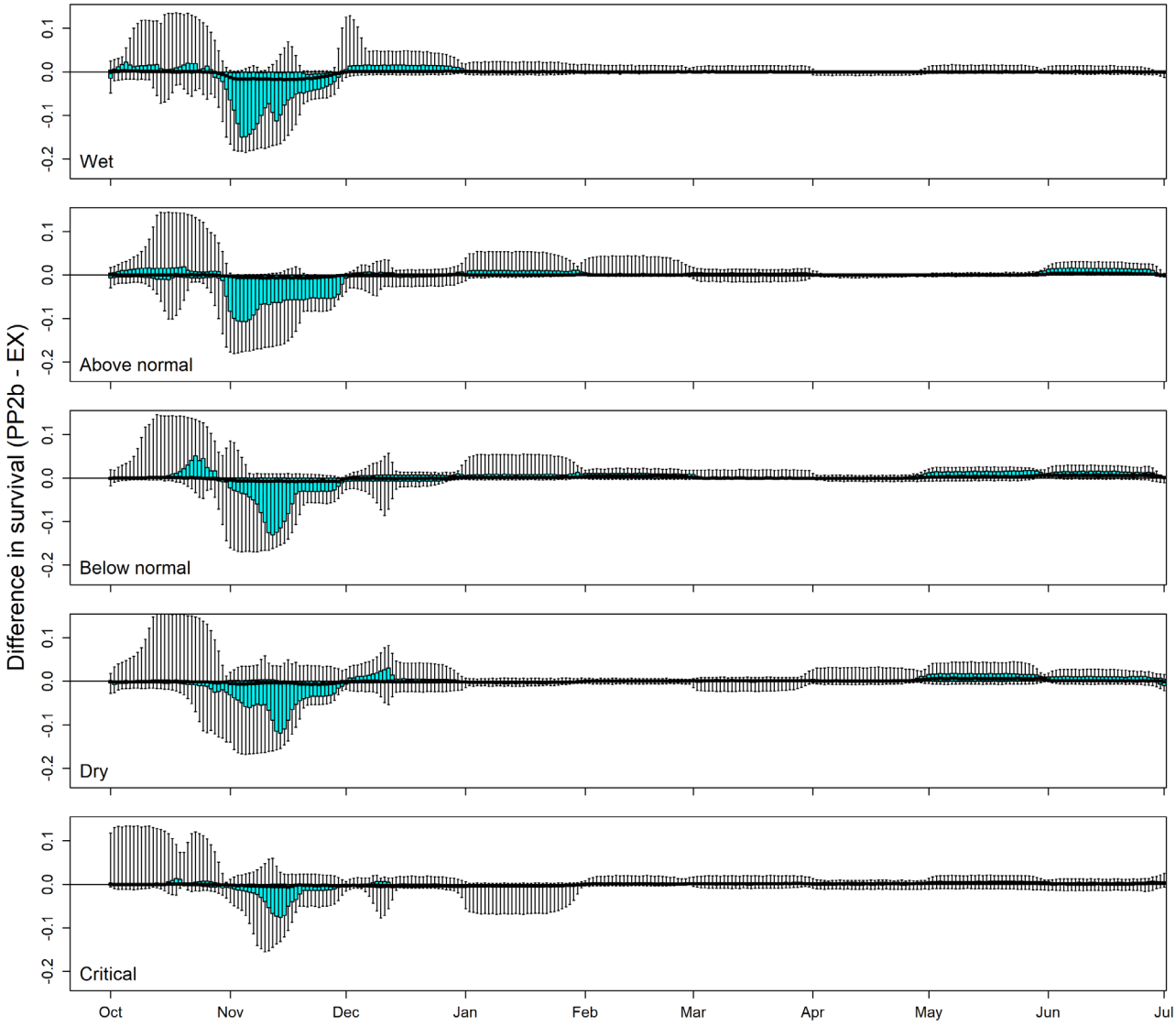


**Figure 28.** Daily boxplots of median differences in through-Delta survival rates between the Proposed Project 2b (PP2b) and Existing (EX) scenarios by water-year type. Each boxplot represents the distribution of median survival differences among the 82 years for a given date. The point in each box represents the median, the box hinges bounding the shaded blue area represent the 25th and 75th percentiles, and the whiskers display the minimum and maximum.

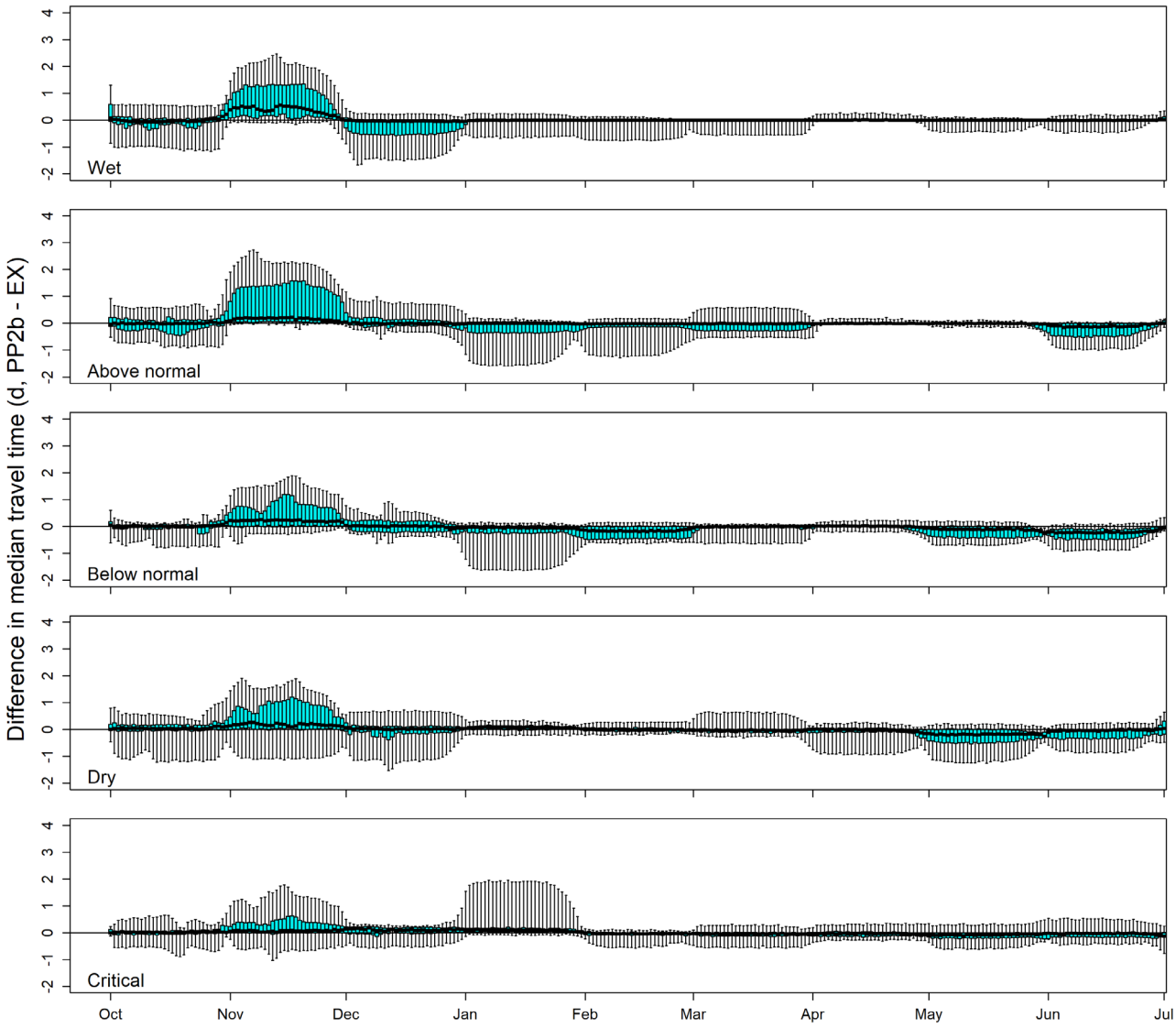


**Figure 29.** Daily boxplots of median differences in median travel time between the Proposed Project 2b (PP2b) and Existing (EX) scenarios by water-year type. Each boxplot represents the distribution of median travel-time differences among the 82 years for a given date. The point in each box represents the median, the box hinges bounding the shaded blue area represent the 25$^{th}$ and 75th percentiles, and the whiskers display the minimum and maximum. d, days.

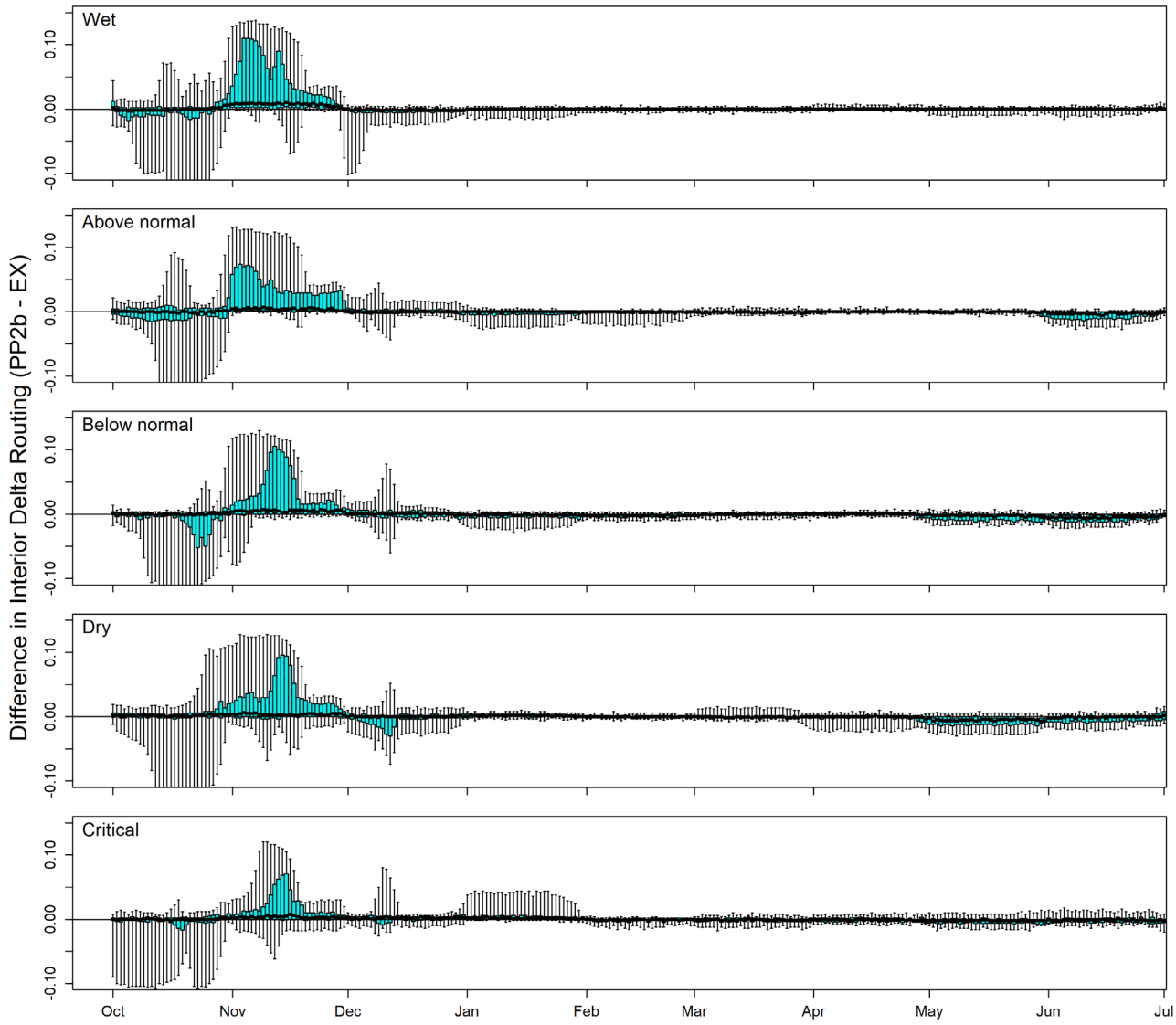


**Figure 30.** Daily boxplots of median differences in routing to the Interior Delta between the Proposed Project 2b (PP2b) and Existing (EX) scenarios by water-year type. Each boxplot represents the distribution of median travel-time differences among 82 years for a given date. The point in each box represents the median, the box hinges bounding the shaded blue area represent the 25th and 75th percentiles, and the whiskers display the minimum and maximum.

## Conclusions

Even though there were operational differences between the two proposed project scenarios, the trends were similar when compared to the EX scenario. Both the PP and PP2b scenarios had lower through-Delta survival, longer travel times, and increased routing to the Interior Delta than the EX scenario during November. In October December, May, and June, the PP and PP2b scenarios were more favorable than the EX scenario, but not substantially. In all months besides November, the median differences between PP and PP2b scenarios and the EX scenario were near 0. The trends between the two proposed project scenarios were similar when comparing by water year, with the greatest differences in the wet and above normal water years when the greatest changes between

scenarios occurs. While the PP and PP2b scenarios were poorer for fish in November than the EX scenario, few winter-run-sized fish are present during this month (del Rosario and others, 2013).

Although our analysis with the STARS model provides insight about potential effects of the PP and PP2b on juvenile salmon migrating through the Delta, several important limitations and assumptions could affect inferences drawn from the model. First, the sole drivers of survival, routing, and travel time in our model are DCC gate position and mean daily inflow to the Delta measured in the Sacramento River at Freeport. Thus, the results we present here are insensitive to other factors that might influence survival and differ between scenarios, such as water exports from the Delta (Newman and Rice, 2002; Newman, 2003; Newman and Brandes, 2010). In addition, the output for daily inflow into the Sacramento River was disaggregated from the monthly flows output by CalSim II by using a constant value of the daily flow each month and smoothing the end-points of each month with a stiff spline. Thus, the STARS model results here display spurious jumps in the mean travel times and survival rates. Whereas these are smoothed somewhat by the averaging process for all the fish ensembles, care should be taken while interpreting the results of the model. This is not a model limitation; rather, it is a manifestation of the adopted scenario-design protocol.

Second, care should be taken when extending inferences beyond the range of data used to fit the model. Observed flows for the analysis conducted by Perry and others (2018) encompassed the 1st–95th percentiles of historical flow, bolstering inferences from the model about the effect of inflows; however, we note that the inflows, water export, and DCC gate operations in almost all the PP, PP2b and EX scenarios are within the range of data used to build the STARS model. Third, the model was fit to large hatchery-origin late-fall Chinook salmon smolts that migrated through the Delta during December through March, yet inferences were extended to all runs over the entire migration period (Perry and others, 2010; Michel and others, 2015). Thus, survival of other runs at other times of the year could have a different response to operations under either of the proposed projects. Last, because our model was fitted to juvenile-salmon telemetry data for the years 2005–2011, it is a representation of the Delta in its current state, not some future state. Because our model characterizes the relation between Delta inflows and survival in the present-day Delta, it is insensitive to future changes to the Delta that modify the relation between inflows and survival. For example, Perry and others (2018) identified the strongest flow-survival relations in reaches that transitioned from bidirectional tidal flows at low inflows to unidirectional river flow at high inflow, implicating tides as an important driver of the flow-survival relation. Future sea-level rise due to climate change will likely alter tidal dynamics in the Delta, and in turn, could modify the relation between inflow and survival. Our model is insensitive to these types of changes to a future Delta.

Given these caveats, our analysis was able to (1) provide a comprehensive assessment of the proposed project by quantifying relative changes in key population metrics between scenarios, (2) identify the magnitude of these changes at given inflows and times of the year, and (3) shed light on mechanisms driving differences between alternative management scenarios. Ultimately, these analyses and others completed for the Incidental Take Permit will result in the development of coordinated long-term operations of the SWP in a manner which minimizes the effects on listed species while facilitating water use that benefits the State of California and the nation.

## References Cited


del Rosario, R.B., Redler, Y.J., Newman, K., Brandes, P.L., Sommer, T., Reece, K., and Vincik, R., 2013, Migration patterns of juvenile winter-run-sized Chinook salmon (*Oncorhynchus tshawytscha*) through the Sacramento-San Joaquin Delta: San Francisco Estuary and Watershed Science, v. 11, no. 1, 22 p., https://doi.org/10.15447/sfews.2013v11iss1art3.

ICF International, 2016, Biological assessment for the California WaterFix: Prepared for the Bureau of Reclamation, Sacramento, California, ICF 00237.15., 62 p.

Kapahi, G., Baer, I., Farwell, J., Riddle, D., and Wilson, G., 2006, Water quality control plan for the San Francisco Bay/Sacramento-San Joaquin Delta Estuary: Sacramento, California, State Water Resources Control Board, 49 p.

King, R., Morgan, B., Gimenez, O., and Brooks, S., 2010, Bayesian analysis for population ecology: Boca Raton, Florida, CRC Press, 456 p.

Michel, C.J., Ammann, A.J., Lindley, S.T., Sandstrom, P.T., Chapman, E.D., Thomas, M.J., Singer, G.P., Klimley, A.P., and MacFarlane, R.B., 2015, Chinook salmon outmigration survival in wet and dry years in California's Sacramento River: Canadian Journal of Fisheries and Aquatic Sciences, v. 72, no. 11, p. 1749–1759, https://doi.org/10.1139/cjfas-2014-0528.

National Marine Fisheries Service (NMFS). 2009. Biological opinion and conference opinion on the long-term operations of the Central Valley Project and State Water Project. National Marine Fisheries Service Southwest Region, 844 p. accessed May 29, 2019, at https://www.westcoast.fisheries.noaa.gov/central_valley/water_operations/ocap.html.

Newman, K.B., 2003, Modelling paired release–recovery data in the presence of survival and capture heterogeneity with application to marked juvenile salmon: Statistical Modelling, v. 3, no. 3, p. 157–177, https://doi.org/10.1191/1471082X03st055oa.

Newman, K.B., and Rice, J., 2002, Modeling the survival of Chinook salmon smolts outmigrating through the lower Sacramento River system: Journal of the American Statistical Association, v. 97, no. 460, p. 983–993, https://doi.org/10.1198/016214502388618771.

Newman K.B., and Brandes P.L., 2010. Hierarchical modeling of juvenile Chinook salmon survival as a function of Sacramento-San Joaquin Delta water exports. North American Journal of Fisheries Management 30:157–169. doi: http://dx.doi.org/10.1577/M07-188.1

Perry, R.W., 2010, Survival and migration dynamics of juvenile Chinook salmon (*Oncorhynchus tshawytscha*) in the Sacramento-San Joaquin River Delta: Seattle, University of Washington, School of Aquatic and Fishery Sciences, Ph.D. dissertation, 223 p.

Perry, R.W., Skalski, J.R., Brandes, P.L., Sandstrom, P.T., Klimley, A.P., Ammann, A., and MacFarlane, B., 2010, Estimating survival and migration route probabilities of juvenile Chinook salmon in the Sacramento-San Joaquin River Delta: North American Journal of Fisheries Management, v. 30, no. 1, p. 142–156, https://doi.org/10.1577/M08-200.1.

Perry, R.W., Brandes, P.L., Burau, J.R., Klimley, A.P., MacFarlane, B., Michel, C., and Skalski, J.R., 2013, Sensitivity of survival to migration routes used by juvenile Chinook salmon to negotiate the Sacramento-San Joaquin River Delta: Environmental Biology of Fishes, v. 96, nos. 2–3, p. 381–392, https://doi.org/10.1007/s10641-012-9984-6.

Perry R.W., Romine J.G., Adams N.S., Blake A.R., Burau J.R., Johnston S.V., and Liedtke T.L., 2014, Using a non-physical behavioral barrier to alter migration routing of juvenile Chinook salmon in the Sacramento-San Joaquin River Delta: River Research and Applications, v. 30, no. 2, p. 192–203, https://doi.org/10.1002/rra.2628.

Perry R.W., Brandes P.L., Burau J.R., Sandstrom P.T., and Skalski J.R., 2015, Effect of tides, river flow, and gate operations on entrainment of juvenile salmon into the interior Sacramento–San Joaquin River Delta: Transactions of the American Fisheries Society, v. 144, no. 3, p. 445–455, https://doi.org/10.1080/00028487.2014.1001038.

Perry, R.W., Pope, A.C., Romine, J.G., Brandes, P.L., Burau, J.R., Blake, A.R., Ammann, A.J., and Michel, C.J., 2018, Flow-mediated effects on travel time, routing, and survival of juvenile Chinook salmon in a spatially complex, tidally forced river delta: Canadian Journal of Fisheries and Aquatic Sciences, v. 75, no. 11, p. 1886–1901, https://doi.org/10.1139/cjfas-2017-0310.

USBR, 2019, Reinitiation of Consultation on the Coordinated Long-Term Operation of the Central Valley Project and State Water Project: Final Biological Assessment, 871 p., accessed May 29, 2019, at https://www.usbr.gov/mp/bdo/lto.html.

Zabel, R. W., 2002., Using “travel time” data to characterize the behavior of migrating animals: The American Naturalist, v. 159, no. 4, p. 372–387, https://www.jstor.org/stable/10.1086/338993.

## Appendixes

Appendixes 1–4 are Adobe Acrobat® files and are available for download at https://doi.org/10.3133/ofr20191127.

**Appendix 1. Simulated Daily Survival by Year, Existing Operations Compared to Proposed Project Scenarios, 1922–2003**

**Appendix 2. Simulated Daily Travel Time by Year, Existing Operations Compared to Proposed Project Scenarios, 1922–2003**

**Appendix 3. Simulated Daily Routing by Year, Existing Operations Compared to Proposed Project Scenarios, 1922–2003**

**Appendix 4. Simulated Proportion of Fish Entering the Interior Delta by Year Existing Operations Compared to Proposed Project Scenarios, 1922–2003**

**Appendix 5. Simulated Daily Survival by Year, Existing Operations Compared to Proposed Project 2b Scenarios, 1922–2003**

**Appendix 6. Simulated Daily Travel Time by Year, Existing Operations Compared to Proposed 2b Project Scenarios, 1922–2003**

**Appendix 7. Simulated Daily Routing by Year, Existing Operations Compared to Proposed Project 2b Scenarios, 1922–2003**

**Appendix 8. Simulated Proportion of Fish Entering the Interior Delta by Year Existing Operations Compared to Proposed Project 2b Scenarios, 1922–2003**

Publishing support provided by the U.S. Geological Survey
Science Publishing Network, Tacoma Publishing Service Center

For more information concerning the research in this report, contact the
Director, Western Fisheries Research Center
U.S. Geological Survey
6505 NE 65th Street
Seattle, Washington 98115-5016
https://www.usgs.gov/centers/wfrc

ISSN 2331-1258 (online)
https://doi.org/10.3133/ofr20191127